Progress in Organic Coatings 154 (2021) 106156

Contents lists available at ScienceDirect

Progress in Organic Coatings

journal homepage: www.elsevier.com/locate/porgcoat

Review

UV-curable waterborne polyurethane coatings: A state-of-the-art and recent advances review

Lucas Dall Agnol [a,*], Fernanda Trindade Gonzalez Dias [b], Heitor Luiz Ornaghi Jr. [c], Marco Sangermano [d], Otávio Bianchi [a,e,*]

[a] Postgraduate Program in Materials Science and Engineering (PGMAT), University of Caxias do Sul (UCS), Caxias do Sul, RS, Brazil
[b] Postgraduate Program in Technology and Materials Engineering (PPG-TEM), Federal Institute of Education, Science and Technology of Rio Grande do Sul (IFRS), Campus Feliz, RS, Brazil
[c] Federal University for Latin American Integration (UNILA), Foz do Iguaçu, Parana, Brazil
[d] Department of Applied Science and Technology, Politecnico di Torino, C.so Duca Degli Abruzzi 24, Turin, 10129, Italy
[e] LAPOL- Department of Materials Engineering (DEMAT), Federal University of Rio Grande do Sul (UFRGS), Porto Alegre, RS, Brazil

ARTICLE INFO

Keywords:
Waterborne polyurethane acrylate
UV-curable
Photocurable waterborne
Polyurethane/acrylate dispersion
Systematic review

ABSTRACT

Waterborne polyurethane coatings prepared by UV-induced photoreactions (UV-WPU) are becoming very attractive due to the increasingly stringent environmental demands. They were developed to replace solvent-based polyurethanes in the coatings of wood, paper, plastics, metal, and glass, mainly because of their good physicochemical, rheological, and optical properties. Several UV-WPU formulations have been tested over the years, making their research substantial. However, no valuable review of this literature, focusing on the significant influencing factors in UV-WPU's manufacture, is available to date. This work aims to answer specific questions about the state of these materials' art, such as: "which monomers have been used most in UV-WPU synthesis?", "what type of photo-initiator has promoted the most efficient curing of the material?", "what additives or particles have been tested for composite UV-WPUs?", "which applications have UV-WPUs been directed to?", "what adaptations and technologies have already been tested to overcome the challenges of the process?", among others. As a result of a systematized bibliographic search in four databases, considering the period from January 2000 to July 2020, a total of one hundred and thirty-eight distinct and relevant articles on UV-WPUs were found. From this study, we hope to present a scientific source on the current state-of-the-art of UV-WPU synthesis, providing new combinations of raw materials and intelligent solutions, thus making material and industrial engineers able to mitigate the inconveniences of the process.

1. Introduction

Polyurethanes (PU) are high-performance materials with a wide range of industrial applications [1,2], mainly due to their tunable physicochemical properties. They are block copolymers produced from the step-growth polymerization reaction between a di/polyisocyanate and alcohol groups (diols), resulting in repeated urethane groups. Since there are differences in the solubility parameters of the PU's block segments, they are thermodynamically incompatible, contributing to phase separation and a structure composed of microdomains [3,4]. Generally, the hard segments derived from the diisocyanates groups contain urethane or urea domains with strong hydrogen bonding and low-molar mass chain extenders. The hard segments of PU are responsible for providing mechanical resistance to the polymeric film, unlike the soft segments derived from polyols, which account for its impact properties [5,6]. The chemical composition of PU in terms of the balance between rigid and flexible blocks will determine the polymer's final properties.

Regarding environmentally friendly PU-based materials, waterborne polyurethane (WPU) appears with low levels of volatile organic compounds (VOCs) and the absence of isocyanate residues. WPUs are widely used as films and adhesives, especially in ecological coatings, as a substitute for traditional solvent-borne ones [7–9]. In polyurethane aqueous dispersions, the particles tend to present 10–300 nm sizes and high surface energy [8,10]. The main difference between solvent-based PU and WPU is hydrophilic segments' presence in the polymer backbone,

* Corresponding authors at: Postgraduate Program in Materials Science and Engineering (PGMAT), University of Caxias do Sul (UCS), Caxias do Sul, RS, Brazil.
E-mail addresses: agnol.lucasdall@gmail.com (L. Dall Agnol), otavio.bianchi@gmail.com (O. Bianchi).

https://doi.org/10.1016/j.porgcoat.2021.106156
Received 21 November 2020; Received in revised form 10 January 2021; Accepted 18 January 2021
Available online 3 March 2021

derived from a diol containing an acid group (such as carboxylic acid, sulfonate, or quaternary ammonium salt) that acts as an internal emulsifier [11]. Although the hydrophilic groups endow excellent colloidal stability, they cause adverse effects to surface properties, water resistance, and long-term performance of WPU-based materials [12,13]. Several strategies can be employed to overcome these inconveniences, such as blending, cross-linking, copolymerizing, grafting of hydrophobic monomers, or incorporating nanofillers to WPU [14–19]. Among these approaches, the cross-linking proved to be most promising because it is based on incorporating acrylic double bonds to WPU, which allows UV curing through chain polymerization [12,20]. The presence of crosslinks provides thermoset coatings with high chemical stability, enhanced tensile strength, excellent abrasion, acid-alkali, solvent resistance, and cure selectively limited to the irradiated area [21–23]. Nonetheless, there are some limitations to this system. Firstly, water has to be driven out of the film by conventional dryers, microwave dryers, and/or IR lamps before UV curing, thus resulting in longer drying times and higher energy consumption can be required [24]. In addition, the density of photosensitive groups of the existing photo-curable resins can influence the film's performance. Depending on the content of these groups in the polymeric matrix, the hardness of the coating films can be poor, and the UV curing rate may be slow, which limits its practical applications in some fields [25].

There are several methods for preparing UV-WPU coatings, such as physical blending, emulsion polymerization, and the interpenetrating polymer network (IPN)-based technique [26–30]. The most conventional method is to end-chain polyurethane with a single-hydroxyl acrylate or to introduce a double bond from hydroxyl-terminated polybutadiene, or even to incorporate vinyl groups into the polymer [31]. UV-WPU dispersions are usually prepared by acetone methods using a three-step procedure, as shown in Fig. 1. In the first step, an excess of a difunctional diisocyanate is reacted with a polyol and end-capped with a hydroxyl (meth)acrylates synthesized in acetone. A part of the chain extender is replaced by a carboxylic acid functionalized diol to improve dispersibility in water. In the second step, the carboxylic acid is neutralized, and the acrylic end-capped polyurethane is dispersed

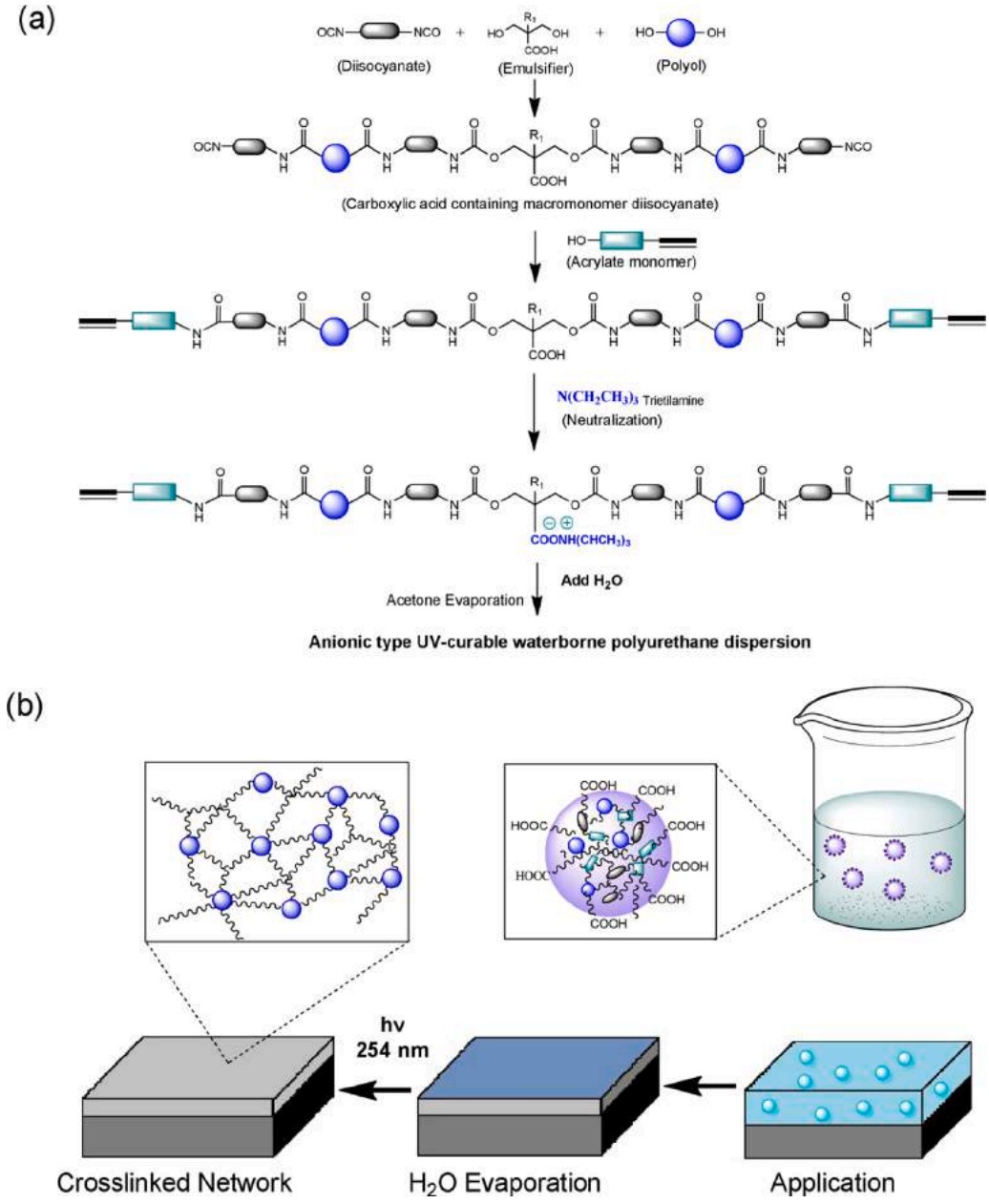

Fig. 1. (a) Reaction scheme for UV-WPU synthesis and (b) schematic illustration of the film formation.

in water. Finally, acetone is removed under vacuum to obtain a WPU dispersion that can give rise to a free-radical type UV curing step. Typically, the urethane dispersion has a pH 7–8 and a solids content of 30–40 wt.%, remaining stable for several months [32]. Since the viscosity of polymeric dispersions is dependent on the concentration and particle size of the chains, it is possible to obtain systems with viscosities suitable for specific applications [33].

Before applying the UV-WPU dispersions on a substrate, the photopolymerizer is added to the solution, which is then exposed to a temperature for the evaporation of water. The ultraviolet light absorbed by the photoinitiator produces free radicals that promote the reaction between the prepolymer and the reactive monomers or diluents, generating the cured films. The dispersion stability and particle size, in addition to the product's final properties, will be influenced by the ionic group's content, rigid/flexible segments molar ratio, structure of the monomers, neutralization degree, acrylate double bond percentage, curing conditions, photoinitiator amount, and others. Moreover, the reaction parameters, such as temperature, stirring, component's feeding rate, and order of addition, significantly affect the aqueous dispersion properties [3,34]. Monitoring the nanoparticle morphology produced in the synthesis is essential to control the interconnected network resulting from its aggregation, which will directly affect the quality of the PU film formed [10]. The film formation by the nanoparticles' aggregation is a complex phenomenon, due to the occurrence of simultaneous physicochemical processes, such as water evaporation, cross-linking reactions, phase separation, droplet coalescence, and others [35]. Thus, to obtain the best physical and mechanical properties of the UV cured product, one must consider the materials used and the conditions under which the film was formed. The reaction conditions will control the polymerization and the double bond conversion in the system.

So far, there was insufficient data reported in the literature on the correlation between polymeric structure, water-resistance, and coating performance for UV-curable WPU systems [25,36]. Therefore, this review aimed to synthesize and discuss the information found in articles published in the Scopus, Web of Science, Science Direct, and Google Scholar databases from 2000 to 2020. As the preparation method of the aqueous PU dispersions is more consolidated in the literature [1,5,25,34,36–39], this study sought to focus specifically on the effect of formulation components on the final properties of UV-crosslinked films.

2. Review methodology

The publications were searched using the Scopus (https://www.scopus.com), Web of Science (https://www.webofknowledge.com), Science Direct (https://www.sciencedirect.com), and Google Scholar (https://scholar.google.com.br) online databases. The keywords employed were: (("waterborne polyurethane" OR "polyurethane acrylate dispersion" OR "polyurethane dispersions" OR "waterborne UV") AND ("UV curable" OR "UV cured" OR "photocurable" OR "ultraviolet curable" OR "UV crosslinking")). The search was limited to English language articles published from January 2000 to July 2020. The publications found were analyzed, while duplicate articles, revisions, or articles that did not produce UV-WPU, were excluded from the results. Articles of polyurethane acrylates that do not perform UV curing and articles that do not detail the UV-WPU composition were only used to support the review's discussion. Considering these criteria, a total of one hundred and thirty-eight (138) relevant publications were detected in the databases search, as shown in Table 1 and mandatorily cited in this review. The parameters analyzed in the eligible articles were: UV-WPU composition, UV curing process, and final properties/application. The other references cited here were also used to support the review's discussion.

3. Literature analysis

The systematic literature research provided remarkable findings among the 138 articles selected. Table 1 summarizes the compositional characteristics, properties, and the leading applications for the UV-WPU systems reported in the analyzed literature. The variety of possible monomer combinations for WPU synthesis was impressive. From the 138 reviewed papers, twenty-seven (27) used polytetramethylene glycol (PTMG) as polyol [26,40–66]. Polypropylene glycol (PPG) was the second most chosen polyol, being part of twenty two studies [12,23,32,40,52,59,65,67–82], followed by poly(ethylene glycol) (PEG) (sixteen studies) [7,21,73,83–96], poly(ε-caprolactone) (PCL) (thirteen studies) [6,20,31,52,59,97–105], polyether diol (twelve studies) [22,106–117], polycarbonate diol (PCD) (ten studies) [24,33,52,103,118–124], and hyperbranched aliphatic polyester (HBP) (nine studies) [11,125–133], vegetable oil (castor, linseed or cardanol) (six studies) [134–139], as well as a mixture of two polyols [65,140,141]. Other polyols were also reported [9,40,73,103,142–152]. Regarding the isocyanate monomer, Table 1 shows that the most used for the UV-WPU synthesis is the isophorone diisocyanate (IPDI). Other diisocyanates also employed were toluene diisocyanate (TDI), 4,4-methylene dicyclohexyl diisocyanate (H_{12}MDI), hexamethylene diisocyanate (HDI), and methylene diphenyl 4,4-diisocyanate (MDI). Concerning the emulsifier, 2,2-bis(hydroxymethyl)butyric acid (DMBA), and 2,2-bis(hydroxymethyl) propionic acid (DMPA) were the most utilized. Triethylamine (TEA) was the most reported agent to neutralize the acid groups of the emulsifier. In a reaction between an isocyanate and alcohol, it is common to use catalysts to accelerate the reaction rate and avoid high temperatures. For the synthesis of WPUs, organotin compounds were adopted, especially the dibutyltin dilaurate (DBTDL). The 2-hydroxyethyl acrylate (HEA), 2-hydroxyethyl methacrylate (HEMA), and pentaerythritol triacrylate (PETA) were the acrylic monomers most cited for the production of UV-WPU. Other acrylic monomers also used were pentaerythritol diacrylate (PEDA), 2,2-bis(prop-2-enoxymethyl)butan-1-ol (DiAE), 2-hydroxypropyl acrylate (HPA), hydroxypropyl methacrylate (HPMA), and trimethylolpropane monoethylene ether (TMPME). For the synthesis of UV-WPU, inhibitors such as hydroquinone (HQ) or 4-methoxyphenol (MEHQ) were generally added to prevent radical UV-initiated curing of the acrylate monomers during the reaction and storage of the emulsion. Acetone, methyl ethyl ketone (MEK), and N-methyl-2--pyrrolidone (NMP) were the most used solvents to lower the medium viscosity since their removal is facilitated and they do not react with isocyanate during the reaction. Chain extenders and inorganic nanoparticles have also been used to improve the properties of the materials. The choice for the photopolymerizer is restricted to water solubility and photoinitiator's compatibility with resins. Darocur 1173 and Irgacure 2959 are the most common photopolymerizers for the UV-WPU synthesis. Other options are Irgacure 184, Irgacure 500, 2,4,6-trimethylbenzoyldi-phenyl phosphine oxide (TPO), and benzophenone (BPO).

Regarding the characteristics of UV-WPU materials obtained after synthesis, it was possible to observe that their average particle sizes were 60–300 nm, except in specific cases [72,90,96,118,138]. After water evaporation, the films are photocured with a UV light incidence of 40–1000 W during photopolymerization times of 0.1–30 min, contents of up to 98 % of double bond conversion degree are obtained. The produced films' average Pencil hardness is around HB–5H, with tensile strength and elongation reaching 3–25 MPa and 10–400 % values, respectively. Also, the thermal degradation of UV-WPU materials can approach 200–310 °C, and their water absorption decreases to 4–20 % values. The potential application of these materials is covering metal, fabric, and wood surfaces. As previously mentioned, the formulation of an efficient UV-WPU material depends on selecting an appropriate method, the nature of fillers, and the product's final application. Therefore, we discuss here the main findings regarding the composition and properties of UV-curable waterborne polyurethanes from the aforementioned search methodology, described in Table 1, mainly concerning the influence of the formulation and UV light intensity on the mechanical, chemical, and physical properties of WPUs.

Table 1
Composition and properties of the UV-cured WPU selected in the databases search.

Polyol (g/mol)	Isocyanate	Catalyst	Emulsifier	Chain extender/ reactive diluent	Solvent	Acrylic prepolymer	Nanofillers	Neutralizing agent	Inhibitor	Photoinitiator (wt%)	UV light intensity/Curing time	Solid content (wt.%)	Particle size (nm)	Gel content (%)	Hardness	Tensile strength (MPa)	Elongation at Break (%)	Thermal degradation at $T_{10\%}$ (°C)	Water absorbability/(%)	Potential application	Ref.
CO_2-polyol	MDI	–	DMPA	–	MEK	PETA/ HEA	–	TEA	–	(3%) Irg.2959	0.5-2017 mW/cm^2	–	30–96	66–88	–	29–67	9.6–150	–	8–14	–	[9]
DAP (1000–2000)	IPDI	DBTDA	DMPA	BDO	acetone	HEMA	–	TEA	–	(0.3%) Irg.184	200 W 5 min	35%	365–746	58–62	–	–	–	–	–	–	[142]
Desmo 1019–55	IPDI	DBTDL	DMPA	–	acetone	TriSH or DiAE	–	TEA	–	(1–1.5%) Irg.2959	600 mW/cm^2	40%	100–200	99	(Pencil) 7H	23.8	40.5	–	–	–	[143, 144]
DME	IPDI	DBTDL	DMPA	TMPMP	acetone	HEMA	–	TEA	–	(2%)BP O/HCPK	1000 W	30%	380	91–97	(Pencil) 4H–6H	10–19	76–176	263–291	2.3–3.5	Coating	[149]
ETP	IPDI, H_{12}MDI	DBTDL	DMPA	Non-ionic diol	DMF, acetone	HEA or HEMA	SiO_2-MSMA	TEA	–	(3–5%) Irg.2959, Irg.500	1000–2200 W 10 min	33–40%	46–86	92–94	(Pencil) H–5H	–	–	230–316	18–28	–	[147, 148]
HBP (H10–H40)	IPDI, TDI	DBTDL	SAN, DMPA or MA	–	THF or dioxane	HEMA, HEA or HPA	LDH or TMSPM	TEA	HQ or MEHQ	(1–2%) Irg.2959, Dar1173, Run1103	80 W/cm 20–250 s	30–40%	30–458	49–97	(Pencil) 2B–4H	8–22	35–91	200–310	6–35	Coating	[11, 125-133]
PBA (2000)	IPDI	DBTDL	DMPA	TMP	acetone	HEMA, HEA or PETA	SiO_2	TEA	HQ or MEHQ	(3–4%) Irg.184 Irg.2959	200 W 2 min	15–45%	34–82	94–96	(Shore A) 82–91	4.2–28	180–206	250–280	3.3–6.2	–	[9, 103, 145]
PCD (500–2000)	IPDI, TDI, IAAE/ H_{12}MDI	DBTDL	DMPA or DMBA	PDMS, silicone, PEG400, PFPE, TPGDA, PCL/PDMS/PCL or HTPB	MEK or acetone	TMPMe HEMA, HBA, HEA or PETA	SiO_2	TEA	HQ or MEHQ	(3–4%) Dar1173 Irg.2959 Irg.500 Micure HP-8	40–3000 mw/cm^2 20–250 s	15–35%	40–740	62–98	(Pencil) H–4H or (Shore S) 43–57	3–34	20–620	260–350	1.3–28	Coating	[24, 33, 52, 103, 118-124]
PCL (500–2000)	IPDI	DBTDL or Bicat-8113	DMPA or DMBA	DETA, IPDA, PDMS, PETTA, DMEA, MDEA, MPEG, CO,AESO, GAA,EDA	acetone or ethyl acetate	TMPMe HEMA, PEDA, HEA or PETA	SiO_2 with TMSPM, carbon black, gelatin with VTMS or β –CD	TEA or AC	HQ or MEHQ	(1–5%) Dar1173 Irg.2959 Chem-73W-CR	8 W/2 h or 100–3000 W; 0.1–6 min	15–35%	14–150	22–97	(Pencil) HB–3H or (Shore A) 75–91	0.1–38	6–560	200–310	2–36	Coating, textiles printing and surface sizing agents	[6, 20, 31, 52, 59, 97-105]
PEA (2000)	TDI	–	DMPA	TMPTA	NMP	HEMA	SiO_2-DMCS	TEA	–	Irg.2959	1000 W	32%	–	–	Pendulum 0.53–0.62	14–16	77–85	–	–	–	[152]
PEG (400–2000)	IPDI, TDI, HDI	DBTDL	DMPA	TMPTA, TPGDA, MPTES, DEOA, TMP,GMA VHSO, BA, EG, APTES, DETA,	MEK, NMP, DMF or acetone	HEA, HEMA, PETA, DPPA	SiO_2, (SiO_2 with MEMO or MPTS), Me-β-CD, $AgNO_3$ or g-C_3N_4	TEA	HQ or MEHQ	(1–6%) Dar1173, Irg.500, Irg.2022, Irg.2100, Irg.2959, Irg.184, TPO or HCPK	15–1000W, 1–30min or 125–400 mW/cm^2 180 s	30–50%	54–2000	54–98	(Pencil) HB–5H or (Shore A) 65–90	0.4–17	20–483	200–350	1.3–12	Textile industry, antibacterial coating, screen printing ink or food packaging	[7, 21, 73, 83-96]

(*continued on next page*)

Table 1 (*continued*)

				MMA, and E51															
PET	IPDI	T-12	DMPA	–	acetone	HEMA	SiO_2-TEOS	TEA	HQ	(3%) Irg.2959	1000 W 8 min	56%	74–489	–	(Pencil) H–5H	–	–	250–290	8–28	–	[150]
PIDG (2000)	IPDI	DBTDL	DMPA	BDO and EDA	acetone	PETA	ATO-MPS	TEA	–	(3%) Irg.2959	8W/cm 40 s	30%	–	92.7	–	18–38	116–142	–	–	–	[151]
pNGA (600)	IPDI	–	DMPA	DMEAE PET3MP	MEK	PEAE	–	TEA	–	Not specified	20 min	28%	56–126	–	–	–	–	–	–	–	[146]
Polyether diol (1120–3000)	IPDI, TDI	DBTDL	DMBA, DMPA	St-BA, TPGDA, TMPTA, glycerol, HFBMA or BA	acetone, DMF or NMP	HEA, HEMA, PETA, HPA or HPMA	ZnO, GO or SiO_2-GLYMO or TEOS	TEA	HQ or MEHQ	(0–4%) Dar1173, Irg.184, Dar.651 or TPO	800-1000 W 0.1–30 min	20–30%	32–260	42–98	(Pencil) B–H or (Shore A) 51–98	0.7–11.6	10–399	150–310	0.8–22	Coating and electromagnetic shielding	[22, 106-117]
PPG (400–2000)	IPDI, TDI, HDI, H_{12}MDI	DBTDL or DBTDA	DMPA or DMBA	MLGLY, DA_2OH, PMDA, OF-diol, E51, HTPB, TMP,EDA, FDO,BDO, CO, DEG or HZM	MEK or acetone	HEA, HEMA, PETA, DAA-GPTMS	Fe_3O_4-VTMS, h-NZFO, hBN-OH, ATO, HAP with VTMS, SiO_2 or OVPOSS	TEA	HQ or MEHQ	(0.3–5%) Dar1173, Irg.2959, Irg.500, Irg.184, or TPO	1–125 mW/cm^2 2–15min or 8–1000 W; 0.5–120 min	20–48%	26–311	43–98	(Pencil) 3B–4H or (shore A) 52–95	0.6–200	1.5–630	240–290	2–45	Coating and microwave absorbing	[12, 23, 32, 40, 52, 59, 65, 67-82]
PTAd (1000)	H_{12}MDI	DBTDL	DMPA	DA_2OH	–	HEA	–	TEA	–	(3%) Dar1173	Not specified	30%	–	–	(Shore A) 59	38	80	–	14	–	[40]
PTMG (250–2000)	IPDI, HDI, TDI, H_{12}MDI	DBTDL	DMBA, DMPA or AC	DA_2OH, MDEA, PDMS, APTES, PMDA, DHPDMS TMPME, HEG,SMA MMA, BA, BDO, Gly, TETA, PE, TMP or HFIP	acetone, DMAC, MEK or NMP	HEA, HEMA, PETA, GAP or PEDA	SiO_2, Na^+ montmorillonite with VTMS, C-TiO_2/rGO, (SiO_2 with PEGMA or allyl isocyanat)	TEA	HQ or MEHQ	(1–4%) Dar1173, Irg.2959, Irg.184, Irg.500, Cyr6974, BPO or TPO	8–2000 W 1–120 min	20–50%	97–387	73–97	(Pencil) B–2H or (Shore A) 43–96	0.3–49	90–1120	200–340	0.6–61	Coatings and Self-cleaning coating	[26, 40-66]
PTHF (1000)	IPDI	DBTDL	DMPA	TMP	acetone	HEMA	–	TEA	–	(3%) Dar1173	65 min	30%	–	89–94	(Pencil) 2–3H	–	–	–	6–12	–	[73]
Vegetable oil (castor, linseed or cardanol)	IPDI, HDI	DBTDL	DMPA, MDEA	BDO, TPGDA, TMPTA, DPGDA or HDDA	MEK or acetone	HEA or HEMA	O-MMT or lysozyme	TEA or AC	HQ or MEHQ	(2–3%) Dar1173, Irg.2959 or BPO/HCPK	40–1000W; 0.1–10 min	20–45%	61–5001	53–94	(Pencil) 2H–7H	0.8–21	6–525	187–300	0.8–19	Coating	[134-139]
HMBT/PEUDA	IPDI	DBTDL	DMPA	TMPTA, HDDA	acetone	HEA	–	TEA	MEHQ	(3%) Irg.2959	300W/in 0–250 s	30%	41–69	18–80	Pendulum 35-128	–	–	260–290	4–23	Coating	[140]
PEO/PPO/PEO (2000)	IPDI	DBTDL	DMPA	–	acetone	HEMA	SiO_2	TEA	HQ	(3–4%) Irg.2959	200 W 2 min	30%	31–34	–	–	0.4–0.9	300–400	–	–	–	[65]
PEA/PPO (400–2000)	IPDI/MDI	DBTDL	DMPA	DPHA, DPGDA	–	PETA or HEA	–	TEA	–	(3%) Irg.184	1000 W 15 s	42%	64–104	–	(Pencil) 4H–4H	–	–	250–315	2.5–25	Coating	[141]

AC: acetic acid; AESO: acrylated epoxidized soybean oil; APTES: 3-aminopropyltriethoxysilane; ATO: antimony doped tin oxide; BA: butyl acrylate; BDO: 1,4-butane diol; BPO: benzophenone; CO: castor oil; DA2OH: 1,3-dihydroxy-2-propanone; DAA-GPTMS: derived from diallylamine with methyldiethoxysilane; DAP: Dimer fatty acid-based polyol; Dar1173: (Darocur) 2-hydroxy-2-methylpropiophenone; Dar651: (Darocur 651) Benzil dimethyl ketal; DBTDA: dibutyltin diacetate; DBTDL: dibutyltin dilaurate; DEG: diethylene glycol; DEOA: diethanolamine; Desmo1019-55: poly(hexylene adipate-isophthalate) polyester diol; DETA: diethylene triamine; DHPDMS: dihydroxybutyl terminated polydimethylsiloxane; DiAE: 2,2-bis(prop-2-enoxymethyl)butan-1-ol; DMAC: N,N-Dimethylacetamide; DMBA: 2,2-bis(hydroxymethyl)butyric acid; DMCS: dimethyl dichlorosilane; DME: dimer acid-modified epoxy polyol; DMEA: N,N-dimethyl ethanolamine; DMF: N, N-dimethyl formamide; DMPA: 2,2-bis(hydroxymethyl) propionic acid; DPGDA: dipropylene glycol diacrylate; DPHA: dipentaerythritol hexaacylate; DPPA: dipentaerythritol pentaacrylate; EDA: ethylene diamine; EG: ethylene glycol; ETP: ester-type polyol; E51: bisphenol-A-based epoxy resin; FDO: fluorinated macromolecular diols; GAA: guanidinoacetic acid; GAP: glycidyl azide polymer; g-C3N4: graphitic carbon nitride; Gly: glycidol; GLYMO: 3-glycidyloxypropyltrimethoxysilane; GMA: glycidyl methacrylate; GO: graphene oxide; HAP: hydroxyapatite; HBA: 2,2-bis (hydroxymethyl) butyl acrylate; hBN-OH: hydroxylated hexagonal boron nitride; HBP: hyperbranched aliphatic polyester; HCPK: 1-hydroxycyclohexyl phenyl ketone; HDDA: hexanediol diacrylate; HDI: 1,6-hexamethylene diisocyanate; HEA: 2-hydroxyethyl acrylate; HEG: 1,6-hexylene glycol; HEMA: 2-hydroxyethyl methacrylate; HFBMA: 2,2,3,4,4,4-hexafluorobutyl methacrylate; HFIP: 1,1,1,3,3,3-hexafluoro-2-propanol;

HMBT: 1,6-Hexamethylene bis(thioglycolic acetate); (H_{12}MDI) 4,4′-dicyclohexylmethane diisocyanate; h-NZFO: Ni0.3Zn0.5Fe2O4 nanospheres; HPA: 2-hydroxypropyl acrylate; HPMA: hydroxypropyl methacrylate; HQ: hydroquinone; HTPB: hydroxyl-terminated polybutadiene; HZM: hydrazine monohydrate; IAAE: isocyanate-functionalized aliphatic acrylic ester; IPDA: isophoron diamine; IPDI: isophorone diisocyanate; Irg.184: (Irgacure) 1-hydroxycyclohexyl phenyl ketone; Irg.2959: (Irgacure) 2-hydroxy-4′-(2-hydroxyethoxy)-2-methylpropion-phenone; LDH: layered double hydroxide; MA: maleic anhydride; MDEA: N-methyl diethanolamine; MDI: methylene diphenyl 4,4-diisocyanate; MEHQ: 4-methoxyphenol or p-hydroxyanisole; MEK: methyl ethyl ketone; MEMO: methacryloxy (propyl) trimethoxysilane; MLGLY: hydrophilic maleic anhydride–glycerol oligomer; MMA: methyl methacrylate; MPEG: methoxypolyethylene glycols; MPS: 3-methacryloxypropyltrimethoxysilane; MPTES: 3-mercaptopropyltriethoxysilane; MPTS: methacryloxypropyltrimethoxysilane; MSMA: 3-(trimethoxysilyl) propylmethacrylate; NMP: N-methyl-2-pyrrolidone; OF-diol: perfluorooctanoate glycerate; O-MMT: organic montmorillonite; OVPOSS: octavinyl polyhedral oligomeric silsesquioxane; PBA: polybutane adipate diol; PCD: polycarbonate diol; PCL: polycaprolactone diol; PDMS: polydimethylsiloxane; PE: pentaerythritol; PEA: poly(neopentylneglycol adipate); PEAE: pentaerythritol allyl ether; PEDA: pentaerythritol diacrylate; PEG: poly (ethylene glycol); PEGMA: poly (ethylene glycol) monomethyl ether methacrylate; PEO-PPO-PEO: Poly(ethylene oxide)-poly(propylene oxide)-poly(ethylene oxide); PET: polyester (adipic acid and neopentyl glycol); PETA: pentaerythritol triacrylate; PETTA: pentaerythritol tetraacrylate; PET3MP: pentaerythritol tetrakis(3-mercaptopropionate); PEUDA: propionic ester-based urethane diacrylate; PFPE: hydroxy-terminated perfluoropolyether; PIDG: polyisophthalic diglycol; PMDA: pyromellitic dianhydride; pNGA: poly(neopentyl glycol adipate); PPG: polypropylene glycol; PTAd: poly(tetramethylene adiphate)glycol; PTHF: polytetrahydrofuran; PTMG: polytetramethylene glycol; Run1103: (Runtecure) 1-(4-Hydroxy-2-methylphenyl)propan-1-one; SAN: succinic anhydride; SMA: surface modifying agent; St-BA: styrene butyl acrylate; TDI: toluene diisocyanate; TEA: triethylamine; TEOS: tetraethoxysilane; TETA: triethylene tetramine; THF: tetrahydrofuran; TMP: trimethylolpropane; TMPME: trimethylolpropane monoethylene ether; TMPMP: trimethylolpropane tris(3-mercaptopropionate); TMPTA: trimethylol propane triacrylate; TMSPM: trimethoxysilyl-propyl methacrylate; TPGDA: tripropyleneglycol diacrylate; TPO: 2,4,6-trimethylbenzoyldi-phenyl phosphine oxid; TriSH: 2,2-bis(3-sulfanylpropanoyloxymethyl)butyl-3-sulfanylpropanoate; VHSO: vinyl hydroxyl silicone oil; VTMS: vinyltrimethoxysilane; β –CD: β-cyclodextrin; Me-β-CD: methylated-β-cyclodextrin.

3.1. Diisocyanates and polyols

3.1.1. Isocyanates

Isocyanates are highly reactive compounds and create chemically different products when combined with active hydrogen (−OH and –NH functional substances), forming urethane and urea groups. Isocyanates aromatic, aliphatic, cycloaliphatic, or polycyclic in their structures prepare WPU coatings. By varying the type or content of diisocyanates, coatings with different properties can be produced [25]. For example, H_{12}MDI or MDI's selection will provide resins with enhanced mechanical properties due to the cyclic structure or benzene rings that these reagents have. On the other hand, by choosing HDI, flexible coatings will be obtained as a result of the long-chain alkane present in this diisocyanate. Using IPDI to control the reaction process favors a distinct chemical structure for compounds due to the different reactivities of the two isocyanate groups present in this reagent at low temperature [25]. Aromatic diisocyanates give more rigid PUs than aliphatic ones, but their oxidative and ultraviolet stabilities are lower [39,153]. Compared with other aromatic isocyanates, IPDI is a favored monomer to prepare WPU, since it shows higher weather resistance, better controllable activity, and more rigidity [71,73]. Comparing the effects of using IPDI or TDI in the same formulation, the IPDI-based UV-WPU dispersion exhibited a more pronounced pseudoplastic behavior than the TDI-based one [92]. Chain entanglement and hydrogen bonding between urethane and urea linkages can be more readily formed in the IPDI-based prepolymer because of its chains' flexibility. However, the TDI-based chain-extended UV-WPU is superior in thermal stability than the IPDI-based counterpart. The incorporation of phenyl into the backbone relatively decreases the rotation of single bonds. Consequently, the molecular chains become more rigid, shifting the glass transition temperature (T_g) to higher temperatures. During coating curing, the conversion for the TDI-based UV-WPU drastically increased to a maximum of 75.4 %, whereas the curing reaction for IPDI-based UV-WPU proceeded more steadily, as shown in Fig. 2(a). This is attributed to the difference in chain mobility. The reduction of the chain mobility caused by the stiffness in the hard segments of the TDI-based UV-WPU also anticipates the autoacceleration due to the gel effect. In contrast, there is a less gel effect during the IPDI-based UV-WPU curing because of its chain flexibility. However, this contrast in the different diisocyanates' curing behavior is attenuated for the UV-WPU from the 2000 g/mol molecular weight polyol [Fig. 2(b)]. This implies that increased soft portions attenuate the diisocyanate segment's effect on chain mobility [53]. A significant difference in the average size of particles formed from UV-WPU formulations prepared with HDI or TDI was observed [58]. While the average particle size of the formulation containing only HDI was 38 nm, the average particle size from the one that used only TDI was 158 nm. It is believed that aromatic rings show a better hardness in macroscopic properties, so the coating hardness increases with the increase of TDI usage.

Environmentally-friendly coatings were also synthesized with different proportions of H_{12}MDI and isocyanate functionalized aliphatic acrylic ester (IAAE). The IAEE promoted an increase in the cured coatings' tensile strength and pencil hardness, while the elongation decreased. This behavior can be associated with the high reactivity of IAAE, which has two isocyanates and two unsaturated functional groups, providing a high crosslink density [121].

3.1.2. Polyols

Polyols, the reaction partners for diisocyanate, are mainly dihydroxy terminated long-chain macroglycols with a wide range of molar masses (M_w = 400–6000 g/mol). There are significantly more commercially available polyols (>500) than isocyanates. Among polyols, polyester and polyether ones are the most used to synthesize UV-WPUs. The use of low molar mass polyols results in stiff polymers due to the high concentration of urethane groups. On the other hand, high molar mass polyols produce polymer chains with fewer urethane groups and more

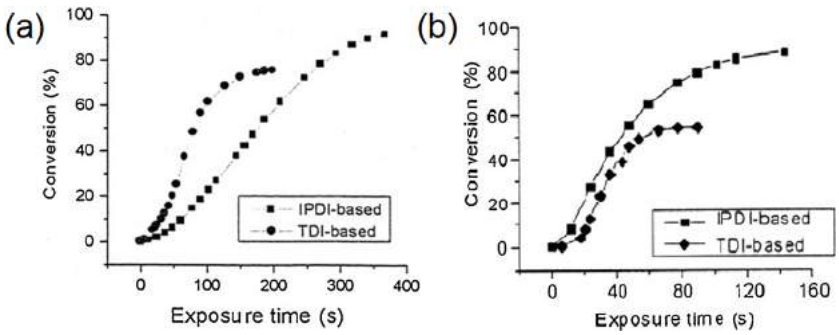

Fig. 2. (a) Effect of diisocyanate type on curing kinetics of chain-extended UV-WPU from PEG 400 g/mol and (b) Effect of diisocyanate type on curing kinetics of chain-extended UV-WPU from PEG 2000 g/mol [92]. Adapted with permission from Ref. 92, Yang J, et al. (2002) J Appl Polym Sci 84:1818–1831. Copyright © 2002 Wiley Periodicals, Inc.

flexible alkyl chains. Long-chain polyols with low functionality (1.8–3.0) give soft, elastomeric PU while short-chain polyols of high functionality (greater than 3) provide a more rigid crosslinked product. Different oligomers' choice directly determines the rigidity of the chain and the hydrophobicity, and viscosity of the polyurethane, resulting in different particle shapes and sizes [37]. The hardness, curing rate, and conversion on the photopolymerization increased with the decrease in the polyol's molar mass, mainly because dispersions based on shorter chain polyols have greater reactivity. A higher relative concentration of methacrylate double bonds in the system forms stronger polymer networks [24,32,56]. Although a higher crosslink density leads to better physical performance, elongation at break is reduced considerably with crosslinking [24,50,118]. High molar mass polyols present larger particle size and lower ionomers weight content in the backbone, leading to higher viscosity systems than polyols of smaller molar mass [106,111,154,155]. Some authors have observed an almost linear correlation between molar mass and average particle size [24,50,59,92], as shown in Fig. 3.

Another interesting fact is that, as the segmental chain length decreases, the segment's movement becomes restricted, and the T_g increases. It is known that polyurethanes possess a two-phase morphology resulting from phase separation between hard and soft segments. The low glass transition temperature (T_{gs}) is attributed to the soft-segment phase, whereas the high glass transition temperature (T_{gh}) is due to the hard-segment phase. UV-WPUs produced with low molar mass polyols showed a single T_g, which meant good miscibility between the hard and soft segments. As the polymer molar mass increases, the phase separation between soft and hard segments becomes more remarkable

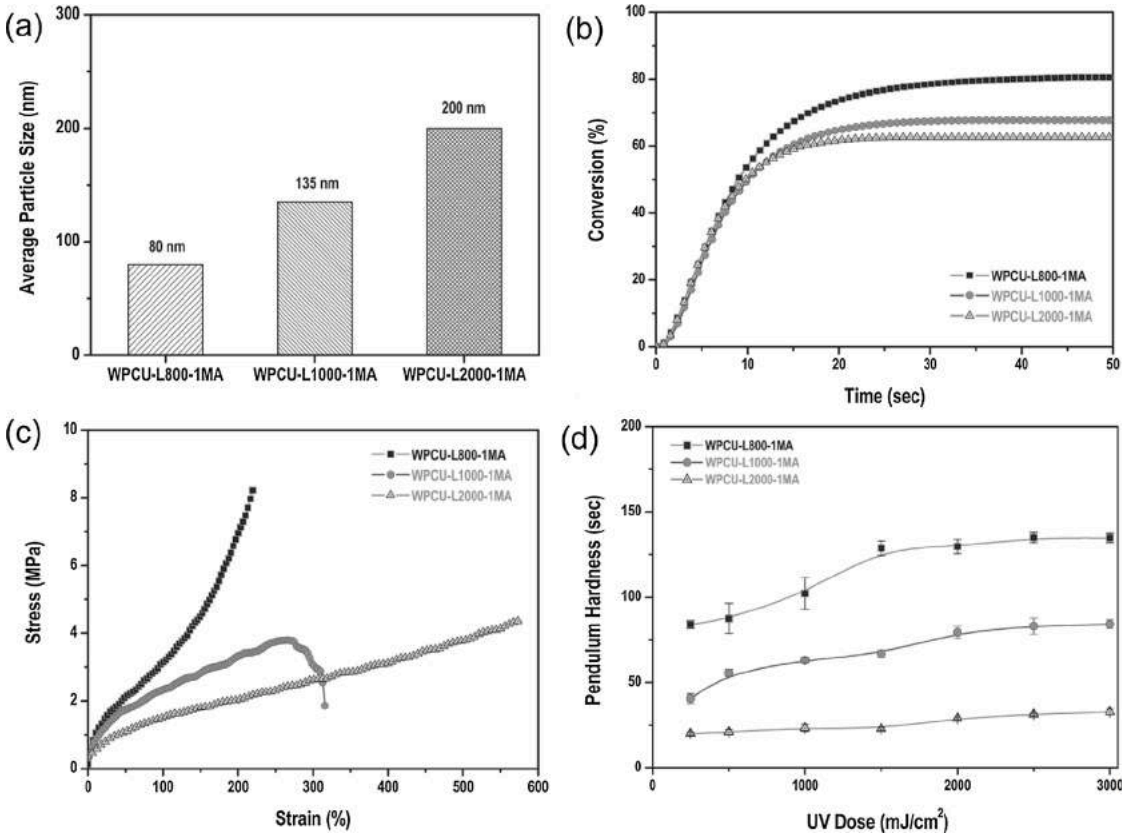

Fig. 3. Effect of molar mass on the properties of a coating synthesized using different PCDs ((■) 800 g/mol; (●) 1000 g/mol; (▲) 2000 g/mol). (a) Average particle size of the dispersion. (b) C═C double bond conversion *vs.* time by photo-DSC. (c) Tensile behavior of the cured film. (d) Pendulum hardness of the cured film as function of the UV-dose [24]. Adapted with permission from Ref. 24, Hwang HD, et al. (2011) Prog Org Coat 72:663–675. Copyright © 2011 by Elsevier B.V.

[92]. Hwang et al. [24] used PCDs with chain lengths of 800, 1000, and 2000 g/mol and obtained T_g values of 44.5 °C, 25.5 °C, and -20.5 °C, respectively. The physicomechanical properties, such as pendulum hardness, maximum tensile strength and glass transition temperature are also affected by polyols' chemical structure due to interactions between inter-chains. Ahn et al. [40], for example, observed that the aliphatic side chain of polymers such as PPG decreased the cohesion forces between groups, resulting in lower mechanical modulus and glass transition temperature. In contrast, polymers such as poly(tetramethylene adiphate)glycol (PTAd) having ester groups show higher values for these properties than PTMG and PPG since the cohesion of the ester groups is higher than that of the ether groups.

The phase separation between hard and soft segments also affects the thermal decomposition of the material. It is known that the thermal decomposition of polyurethane chains has at least two stages. The initial stage at approximately 250 °C is associated with the decomposition of the hard segments, represented by the urea and urethane groups. The second stage at approximately 350 °C denotes the soft segment's decomposition, which involves the polyester and polyether [7,20,21,118]. Conventionally, the molar mass of PU is increased by chain extension of isocyanate-terminated prepolymers with short diols. These chain extensions produce many urethane linkages that are vulnerable to thermal decomposition and limit some applications. Etxaniz et al. [142] observed that the T_g of a formulation prepared by a dimer fatty-acid-based polyol and IPDI shifted to lower temperatures with the increase in the hard segment, due to greater phase separation. Thus, the hard segment's chemical modification is of crucial importance to enhance the thermal stability of UV-WPU. This can be done by introducing thermally stable heterocyclic groups in the hard segment [47]. For example, when the imide groups replaced the urethane groups in the hard segment, remarkably enhanced hardness, tensile modulus, strength, and thermal stability were obtained. The augmented mechanical strength of UV-WPU with the imide hard segment is due to the combined effects of increased hydrogen bondings (one imide group has two carbonyl groups), dipole interactions between imide rings, and the rigid structure of the hard segment [47,61,72].

The polyol plays an essential role in the structure of the molecular chain due to its polarity, which influences the particles' size and the water absorption of the films. Ahn et al. [40] showed that films based on PTAd as soft segments having ester carbonyl hydrogen bonds have higher water swelling than two other types of soft segments, such as PPG, and PTMG. Polyols with regular structures can form crystalline domains more easily, being the cohesive strength between the soft segments so high that it becomes difficult to penetrate water molecules into the membranes [52]. Yoon et al. [59] compared three formulations with the same prepolymer molar mass from different polyols and observed that particle size increased in the order PPG, PTMG, and PCL. This order depended on the difference in solubility parameters between water and polyol, as noted from 8.63 (PCL), 8.90 (PTMG), 12.6 (PPG), and 23.4 (water) $(cal/cm^3)^{1/2}$.

Vegetable oil is being used to replace petroleum products in the preparation of UV-WPUs, mainly due to its low cost and renewable feedstock [25]. UV-WPUs prepared from castor [13,104,134–137], linseed [138], epoxy soybean oil [105], and cardanol [139] polyols showed excellent flexibility, water resistance, hydrolytic stability, shock absorption, and electrical insulation properties. However, the main drawback is their low thermal decomposition temperature. The final double bond conversion of the samples was between 64–80 %. Another disadvantage is the large particle size compared to the WPUs obtained with synthetic polyols using the same content (or higher content) of emulsifier. Bio-based polyols act as an internal emulsifier attributed to the lower polarity of the backbone [142]. In recent years, the hyperbranched polymer has gained increasing attention as a novel type of binder material for waterborne UV-curable ink. Compared to its linear counterpart, the hyperbranched polymer displays low viscosity, high activity, good oxygen resistance ability, excellent compatibility due to its highly branched structure, low intermolecular entanglement degree, and a significant number of end functional groups (increasing the crosslinking density) [25,73,93,129,156,157]. Due to the nature of compactly packed periphery, high density, cross-linking, and lack of chain entanglements, hyperbranched polyurethanes are usually too brittle to form freestanding and mechanical robust films. Incorporating dendritic hyperbranched WPU into the curing system can increase the crosslink density [11,25,93,129,131,132], resulting in films with a highly compact structure due to its functionality. However, although the crosslink density increase has reinforced coatings' rigidity, the decrease in their elongation at break is still noticeable [133,140].

Another type of UV-curable WPUs can be prepared by blending multifunctional thiol- and ene-terminated polyurethane aqueous dispersions. Thiols have been used to reduce the effects of oxygen inhibition by undergoing chain transfer with the peroxy radicals to produce hydrogen peroxide, and thiyl radicals, which can initiate polymerization. The UV-cured polyurethane films prepared by this method also showed increases of 25 % and 10 % in Young's modulus and strength at break values, respectively. However, the coating materials obtained usually have low T_g values and poor mechanical properties due to flexible thio-ether bonds, low cross-linking density, and limited availability of rigid thiol monomers. Also, some unreacted thiol groups in cured polymer networks may be unreacted due to the low reactivity of thiols compared to acrylate groups, leading to a dramatic reduction in

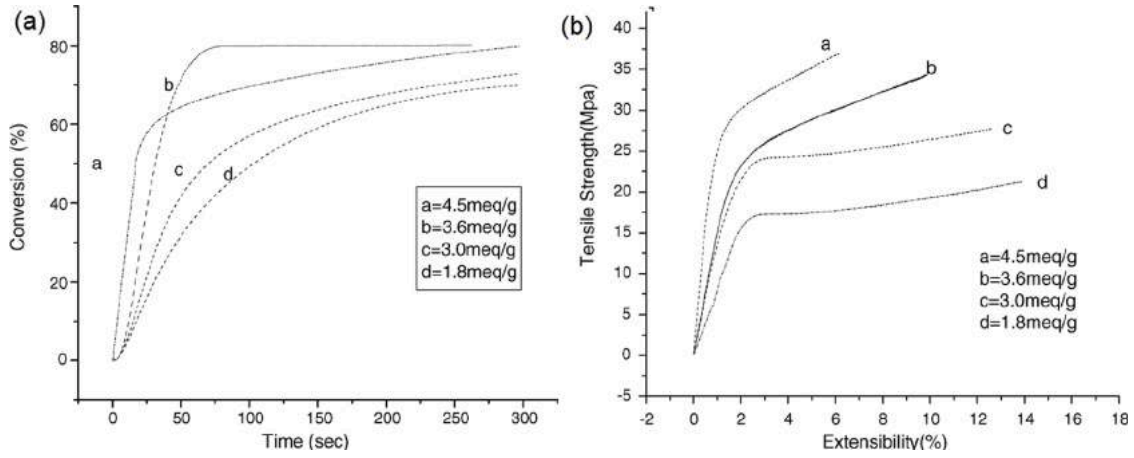

Fig. 4. (a) Conversion comparison for samples containing different C = C contents, using 4% Darocur 2959 and 80 $mW \cdot cm^{-2}$ light intensity. (b) Stress–strain curves of UV-cured waterborne films for the same samples [31]. Adapted with permission from Ref. 31, Bai CY, et al. (2006) Prog Org Coat 55:291–295. Copyright © 2005 Elsevier B.V.

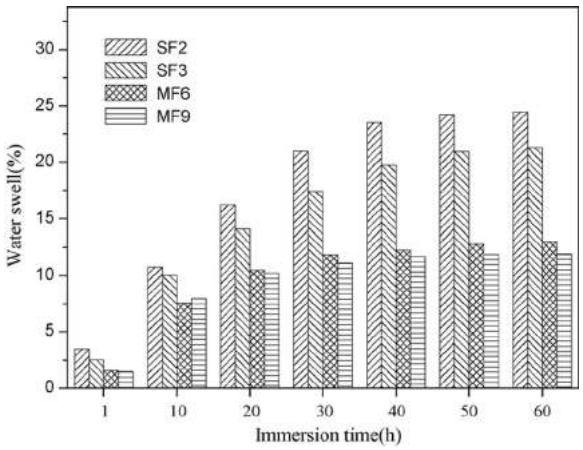

Fig. 5. Water swell percentage *versus* immersion time for UV-WPU films with different C = C contents [6]. Reproduced with permission from Ref. 6, Zhang T, et al. (2010) Prog Org Coat 68:201-207. Copyright © 2010 Elsevier B.V.

performance properties [116,143,144,146,149].

3.2. Influence of the C=C content

There are three most used techniques for incorporating acrylic polymers into WPU dispersions: physical blending, emulsion polymerization, and IPN [26]. The physical blending method involves the independent preparation of the polyurethane and polyacrylate emulsions, followed by their simple mechanical mixing at a certain proportion. This is the simplest way to compound PU and polyacrylate. However, the low compatibility between PU and polyacrylate makes the film susceptible to cracks [158]. In emulsion polymerization, the PU prepolymer's end-capping with hydroxy vinyl monomers (such as hydroxyl acrylates) introduces a double bond into the polymer structure, which is then copolymerized with acrylate monomers. Emulsion polymerization significantly improves water and weather resistances and the transparency of films, being widely used in the synthesis of waterborne coatings [24,50,118]. IPN is a compound polymer, wherein at least one of the components is a network crosslinking structure that is not involved in chemical bonding with the other networks. The emulsion composed of polyurethane-acrylate (PUA) should be synthesized from a PU prepolymer previously prepared. Polyurethane and acrylate form separate microphases, with an interfacial physical crosslinking between them, i.e., there is a three-dimensional "mechanical entanglement" at the interface between phases. Most UV-curable waterborne coatings cannot provide proper water and solvent resistance, nor good mechanical properties, due to their low the C=C content and low molecular weight. Moreover, water absorption disparity is also affected due to the different crosslinking density and chain mobility. The control of the double bond content of the acrylate incorporated into the PU structure greatly influences the polymer's final properties [6,23,31,54,137]. This is mainly because the introduction of acrylate in WPU will significantly change its chain structure and crosslinking density. Indeed, a UV-WPU coating with a higher double bond concentration will provide films with a higher crosslink density after curing [106].

Investigating the UV curing kinetics, Zhang et al. [6] and Bai et al. [31] observed that too high or too low average functionalities were unfavorable for increasing unsaturation conversion. The sample with the highest C=C content (4.5 meq/g) showed the highest initial conversion rate. However, when the radiation time increased, the C=C conversion rate for the sample with 3.6 meq/g C=C became higher than that of the sample with 4.5 meq/g C=C, as shown in Fig. 4(a). This trend can be justified based on the influence of chain mobility. The conversion rate, i.e., the crosslinking rate of the C=C bond, decreased with increased radiation time, mainly due to the molecular chain motion restriction at high crosslinking densities [31,91]. When the average functionality of the UV-WPU is not high, the polymer chains are flexible and active, and the crosslink density can still increase with increasing functional groups. However, when the average functionality of UV-WPU is high enough, the chain movement is restricted, and the remaining active groups are unable to polymerize sequentially, causing the crosslink density to become constant. In this case, the average functionality of UV-WPU will have a minor effect on the crosslink density and its water-resistance [6]. Also, the water swelling disparity is much smaller when the functionality is high (Fig. 5), which can be attributed to the differences in crosslink density and chain mobility.

The thermal stability of the cured film increased by the C = C content. For the samples containing 4.5 meq/g C = C and 1.8 meq/g C = C, the initial decomposition temperatures of 295 °C and 270 °C were observed, respectively. The samples with a higher C = C amount showed a two-stage degradation behavior, which reveals that the decomposition mechanism is dependent on the C = C content [6,31]. Although the increase in C = C content favors the increment of hardness, solvent resistance, tensile strength, and initial mechanical modulus of the samples, it also compromises their extensibility [Fig. 4(b)]. When the C = C content was high [sample a, Fig. 4(b)], the film showed a brittle trend and low extensibility. By reducing the C = C content [samples c and d, Fig. 4(b)], the materials presented a yielding pattern with increasing extensibility and reduced tensile strength and initial modulus [31,118]. Bai et al. [31] reported that a proper UV-curable polyurethane dispersion should have a C = C content of over 2.6 meq/g.

Zhang et al. [6] obtained linear or branched chains by varying the terminal acrylate groups (HEMA or PETA) and the chain extenders (ethylene diamine or diethylene triamine). Thereunto, different UV-WPU samples with different average functionalities were synthesized. As a result, an average controllable functionality of the UV-WPU

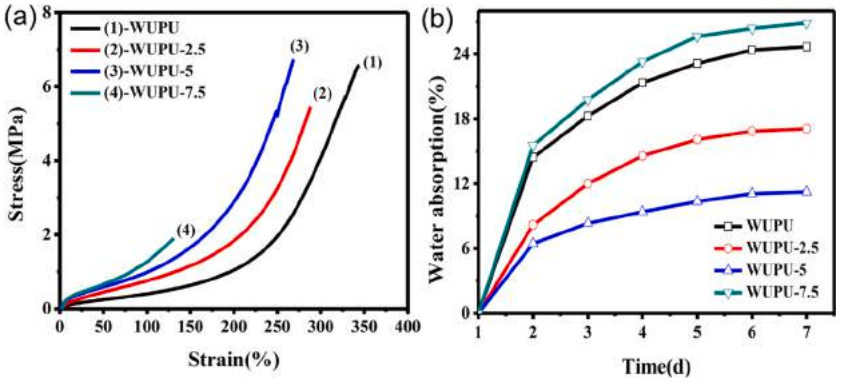

Fig. 6. (a) Tensile behavior and (b) water absorption of APTES-HEA-WPU films. WUPU-x, where x is the mass weight fraction of the APTES-HEA [51]. Adapted with permission from Ref. 51, Zhang S, et al. (2015) Colloids Surf A Physicochem Eng Asp 468:1–9. Copyright © 2014 Elsevier B.V.

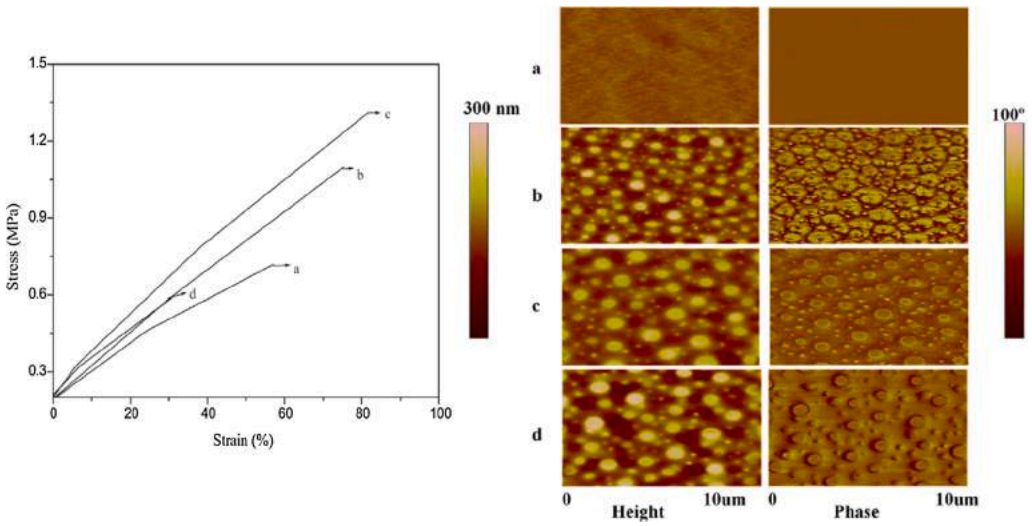

Fig. 7. (a) Stress–strain curves for the hybrid films: (a) UV-WPU, (b) UV-WPU-Silica-5, (c) UV-WPU-Silica-10, (d) UV-WPU-Silica-15; (b) AFM images of topography (left) and phase (right) for: (a) UV-WPU, (b) UV-WPU-Silica -5, (c) UV-WPU-Silica -10, (d) UV-WPU-Silica-15 [88]. Adapted with permission from Ref. 88, S. Zhang S, et al. (2011) Prog Org Coat 70:1–8. Copyright © 2010 Elsevier B.V.

was achieved, reaching up to 9. Consequently, the UV-WPU samples obtained a chemical structure with similar amounts of hard and soft segments, but different crosslinking densities. This difference in the average functionality affected the material's morphology due to different chemical interactions. For the HEMA series samples (functionalities 2 and 3), the hard segments were separated from each other, being considered dispersed in the flexible segments, due to the low values of functionality and crosslinking density. When a tensile force is imposed, the HEMA samples are easily deformed, resulting in protrusions on the fractured surface and great macroscopical flexibility. However, in the PETA series (functionalities 6 and 9), the hard segments can be interconnected, forming a rigid domain system based on sufficient functionalities and crosslinking densities. Thus, PETA samples can hardly be deformed due to their more substantial cohesive energy and covalent bonds. They easily reconvert when the external force is removed, keeping the surface relatively uniform. The replacement of relatively long-distance intermolecular Van der Waals bonds by shorter covalent bonds makes the cured films' shrinkages more significant with the increase in average functionality. This problem can be counteracted by optimizing the curing conditions [6].

Another interesting factor is that acrylate monomers in the WPU formulation can affect the average particle size. When UV-WPUs were produced using the same polyol (PCD 800 g/mol) but with HEA or HEMA acrylate monomers, no significant difference was observed between the particle sizes obtained (78 nm for HEA-based WPU and 80 nm for HEMA-based WPU). However, the average particle size obtained with PETA was much higher (325 nm) than those from the dispersions containing smaller monoacrylate or mono-methacrylate chain end groups. The PETA-based dispersion had bulky tri-acrylate groups at the end of each chain, which increased the dispersion's hydrophobicity, and consequently, altered the particle size [24,101,116,141].

A variation in activity between the tri-acrylate and mono-methacrylate end-cappings was observed. The curing rate and conversion of tri-acrylate functionality are much higher than those samples with mono-methacrylate functionality [33,46,116]. Furthermore, the reactivity of vinyl groups is lower than that of acrylate groups [31]. Hydroxy acrylates with methyl groups, such as HEMA and HPMA, produce UV-WPU oligomeric molecules with higher gel proportions than those prepared from hydroxy acrylates without methyl groups (HEA and HPA) [116]. HEA-terminated WPU showed much lower tensile strength than PETA-terminated WPU. HEA gives much more significant swelling than PETA [121]. This phenomenon is because the methyl group is electron-donating. UV-WPUs that contain methyl groups have a higher reactivity and are UV-cured more thoroughly. However, it should be noted that specific properties of UV-cured films, such as hardness and water resistance, are weak when only monofunctional hydroxyl acrylates are used in UV-WPU's synthesis. This is because the double bond content is too low, and each hydroxyl acrylate group contains only one double bond. In this way, only linear macromolecules are formed as UV-cured films. Meanwhile, there is no network crosslinking macromolecules in UV-cured materials [98,101,116]. Changes in C═C content had no significant effect on UV-curable WPU dispersions' zeta potential, which suggested that the emulsion had proper stability to resist aggregation [69].

3.3. Chain extender and reactive diluents

3.3.1. Chain extenders

Chain extenders are used as additives in the production of UV-WPUs to increase the molar mass of polyurethane and improve their properties [92]. The chemical structure and length of the diol chain extender have a significant effect on polyurethanes' crystallinity and hydrogen bonds degree. Diols containing an even number of methylene groups (i.e., butanediol and hexanediol) improve polyurethane crystallinity compared to diols containing an odd number of such groups (such as pentanediol). The chain extenders most used for UV-WPU dispersions are low molar mass difunctional diols (such as ethylene glycol, 1,4-butanediol, 1,6-hexanediol, etc.), or cyclohexane dimethanol, diamines, hydroxyl-amines, etc. [101]. The addition of functional chain extenders such as polydimethylsiloxane (PDMS) [33,120], fluorinated monomer [48,64,74,77,110,119,159,160], glycidyl azide polymer (GAP), and PTMG [60] can alter the hydrophilicity and free surface energy of the coating, reducing its water absorption. The multifunctional chain extender 1,3-dihydroxy-2-propanone [40] was used as a crosslinking agent to build-up multi-armed polyurethane prepolymers, capable of offering tack-free before cure and peculiar surface and mechanical properties upon curing. Chain extenders with rigid groups such as bisphenol A can significantly improve the coating's hardness and thermal properties. However, benzene rings' introduction may result in the yellowing of coatings, since these functional groups can be easily oxidized into quinones [7,25,85].

Hydroxyl-terminated polybutadiene (HTPB) with two end hydroxyl groups can be used to react with isocyanate. As a soft segment, it will introduce more double bonds to polymer chains. Moreover, as a

polyurethane chain component, HTPB offers the additional properties of resistances to water and low-temperature. Although the increase of HTPB content in the polymer chain harms the formation of a hydrogen bond, a positive effect is observed in the crosslinking density [23,52]. This increase in HTPB content produces an increment in tensile strength, but a decrease in the materials' elongation property. PDMS is another option used in UV-WPU matrices. The PDMS has low surface energy, high flexibility, transparency, and excellent thermal, oxidative, and UV stabilities, therefore giving the UV-WPU films some special properties [33,44,52,54,66,120,123]. However, particularly to the mechanical behavior of the UV-WPU containing PDMS, no significant improvement was observed with the increase in the chain extender content, which was attributed to the high incompatibility between the urethane (or urea) and the PDMS segments from the non-polar nature of the siloxanes. Hydrophobic silicon chains can migrate to the surface layer of the WPU during film formation and UV crosslinking, resulting in many irregular protuberances on the surface of cured films [44,52,66].

The incorporation of PDMS in the WPU reduced the initial speed of light curing, although it did not affect the total conversion at the end of the reaction, that is, the PDMS acted in some way as a curing retardant [33,44,54]. 3-aminopropyltriethoxysilane (APTES) is a kind of multifunctional oligomer with an effect similar to PDMS; it acts as a chain extender during the preparation of UV-WPUs. APTES can increase the nonlinear structure of dispersions. This multifunctional oligomer can hydrolyze into silanol in the aqueous environment and form Si–O–Si linkages by self-condensation reaction of silanol. The increase in the crosslinking density and hydrophobic Si–O–Si bonds, emerging from the addition of APTES in the cured films, directly reflects the reduction of the materials' surface energy. As Si–O–Si bonds have much lower surface energy than polyurethane, they can migrate to the surface during the formation and UV-curing of films, altering their surface properties [21,46,51]. Zhang et al. [51] prepared UV-WPU nanocomposites from a HEA-APTES diol. As shown in Fig. 6(a), a higher crosslinking density is obtained as HEA-APTES content increases, making the systems more rigid, thus reducing the elongation and increasing the modulus. In Fig. 6 (b) the films' water absorption was significantly decreased with increasing the HEA-APTES content to 5.0 %. This may be ascribed to the formation of a hydrophobic and crosslinked siloxane network structure, which prevented the water molecule from entering the bulk film. However, when the quantity is more than 5 wt.%, the films' water absorption was higher than that of neat UV-WPU film. On the one hand, the high content of HEA-APTES led to a decrease in the films' water absorption. Nevertheless, HEA-APTES negatively affected the photo-crosslinking of UV-WPU films. It seemed that the latter factor had a more substantial effect on the crosslink density and water absorption. As a result, a decrease in mechanical performance is observed in the nanocomposite films.

3.3.2. Reactive diluents

Reactive diluents are another kind of additive employed in UV-WPUs production. These additives decrease the curing system's viscosity and help increase the crosslinking density of UV-cured films due to their abundant carbon double bonds [44,141,161]. Consequently, some benefits like high curing rate, low energy consumption, high hardness, and enhanced mechanical properties are obtained. Simultaneously, high crosslinking density can prohibit the water molecular penetrating the inside of films and keep hydrophilic groups from moving towards the surface [141]. Reactive diluents as tripropyleneglycol diacrylate (TPGDA) [124,136], trimethylolpropane triacrylate (TMPTA) [83,96,106,109,137], pentaerythritol [50], pentaerythritol tetraacrylate (PETTA) [100], dipentaerythritol hexaacylate (DPHA) and dipropylene glycol diacrylate (DPGDA) [137,141], modified enzymes [134], trimethylolpropane tris(3-mercaptopropionate) (TMPMP) [149] among others can be added during UV-WPUs synthesis.

Li et al. [100] used PETA as an end-capper and PETTA as a reactive diluent to form PETA/PETTA composite systems, with a more significant amount of unsaturated double bonds, capable of creating films with higher crosslink density. The incorporation of PETTA to the PU molecule created a dense network structure after curing, causing the systems' pencil hardness to increase from 2H to 3H. The PETA/PETTA system's best mechanical properties were obtained for a PETTA content of 35 wt. %. Higher amounts of this reactive diluent produced highly compacted structures with restricted diffusion and motion of PETTA chains or radicals out of networks. Consequently, it brought a reduction of the crosslinking density because of premature termination of polymerization, which was caused by partially unreacted double bonds trapped in polymeric networks. DPHA has higher unsaturation functionality than PETTA and can dramatically increase the crosslinking density in the UV curing process, improving the hardness and water resistance of the resulting films. These properties are fundamental for coatings and paints of consumer electronics, such as mobile phones, CD players, iPods, and others [141].

Xu et al. [22] prepared vinyl-terminated PU prepolymer dispersion through a prepolymer-mixing process and then physically blended it with butyl acrylate (BA) and TPGDA reactive diluents. With the increase of TPGDA content, the hardness of the UV-WPU films rise gradually. This happened because the polarity of the TPGDA was somehow compatible with the rigid PU segment. The increase in the content of TPGDA provided greater impact resistance and hardness to the systems, probably due to the higher hydrogen bond degree; however, the excessive increase in acrylate concentration caused these properties to fall [22,106,109]. When the BA/TPGDA was added, a good dilute effect on emulsion was obtained, reducing the system's viscosity. On the one hand, the molecular motion ability of the UV-WPU emulsion was enhanced, and the C═C quantity was increased. On the other hand, oxygen could spread more easily through the system, which consumed more free radicals, reducing the chances of light polymerization and increasing curing time. The addition of siloxane groups and silane coupling agents can also reinforce the crosslinking density of the system, thus contributing to increase the hardness of the coating [25,122].

3.4. Nanoparticles as a reinforcement component

The incorporation of inorganic nanoparticles into a UV-WPU matrix is an effective strategy to enhance some properties and provide specific functionalities to this system [152]. Hardness, tensile strength, water absorption, solvent resistance, and thermal behavior of UV-WPUs can be significantly improved by adding nanoparticles like acryloyl chloride modified lysozyme [134], silver [90,157], graphene oxide [107,112,113], surfactant-modified TiO_2/reduced graphene oxide [45], graphitic carbon nitride [94], and Fe_3O_4 [70,71]. These nanoparticles also

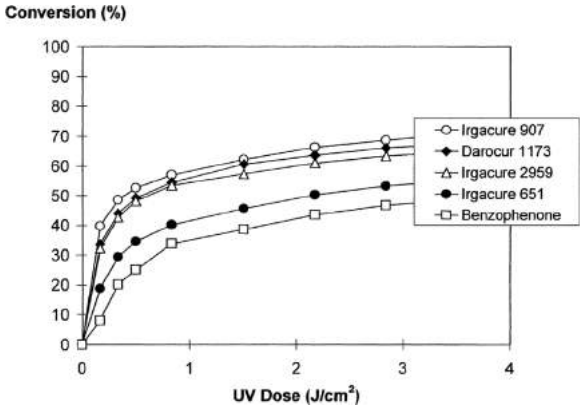

Fig. 8. Influence of the photoinitiator on the UV-curing of a WPU coating. Temperature: 25 °C; light intensity = 60 mW/cm^{-2}; [photoinitiator] = 1 wt.% [165]. Reproduced with permission from Ref. 165, Masson F, et al. (2000) Prog Org Coat 39(2–4) 115–126. Copyright © 2000 Elsevier Science S.A.

provide excellent antibacterial activity, electrical conductivity, good electronic stability, self-cleaning ability in photocatalysis, and unique magnetic behavior to the coatings. However, the homogeneous distribution and dispersion of these materials in the polymer matrix is always a significant challenge. The simple mechanical mixing of inorganic fillers in the polymer matrix is not always effective in preventing agglomeration and poor distribution, which can negatively affect the resulting composites' properties [71,78,103,115]. Considerable efforts have focused on refining the processing techniques (including colloidal-physics [87,120], and *in situ* polymerization [88] methods), and nanoparticle surface functionalization [70,71], silanized polyurethane [123], and *in situ* nanoparticle formation by the sol-gel process [76] to control the proper dispersion of nanosized fillers into WPU matrix. The structure and chemistry of these nanoparticles are essential factors that significantly affect their dispersibility in UV-WPU matrices. Fillers with polar functionalities in their structures, such as epoxy, alkoxy, hydroxyl, acids, amine, and others, are highly dispersible since these groups can interact actively with the polar moieties of the matrix.

The addition of antimony-doped tin oxide (ATO) to a UV-WPU matrix using the sol-gel technique contributed to a better dispersion of the nanoparticles than the same composite prepared by physical blending [76,151]. Besides, the nanoparticle's surface modification was fundamental for achieving good dispersion. The addition of ATO increased the tensile strength of the polyurethane matrix by 317 % compared to the unmodified UV-WPU. Furthermore, the ATO-modified UV-WPU coatings showed a higher initial degradation temperature than the neat UV-WPU coatings, demonstrating improved thermal stability due to the high conversion of C═C bonds (~93 % in 40 s). Coatings containing 3–4 wt% ATO could absorb near-infrared radiation to effectively prevent heat transmission and heat diffusion, increasing the heat-insulating effect.

The functionalizing agents used in the surface modification of nanoparticles, in general, have C═C double bonds, which crosslink by UV-curing, improving the crosslinking density and, consequently, increasing the material properties [70]. The introduction of a siloxane unit to form a cross-linkable PU/siloxane matrix can improve the mechanical and surface hydrophobic properties of UV-WPU films. Some efficient crosslinkers alternatives have been incorporated to UV-WPU dispersions, including dispersions of silane-modified montmorillonite (O-MMT) [135], hydroxyapatite and clay modified by vinyltrimethoxysilane (VTMS) through sol-gel reaction [49,78], hollow $Ni_{0.3}Zn_{0.5}Fe_2O_4$ (h-NZFO) nanospheres functionalized with IPDI and trimethylolpropane [71], trimethoxysilane end-capping agent (DAA-GPTMS) derived from diallylamine (DAA), (3-glycidoxypropyl) methyldiethoxysilane (GPTMS) and modified with edge-hydroxylated boron nitride (hBN-OH) nanosheets [75], vinyltriethoxysilane (VTEO)-modified Fe_3O_4 nanoparticles [70] and octavinyl polyhedral oligomeric silsesquioxane (OVPOSS) [79].

Compared to other inorganic nanofillers, silica nanoparticles have been widely used due to their high hardness, relatively low refractive index, and commercial availability. These nanoparticles can be found as colloidal silica [65,147], aqueous silica sol [88], precipitated or fumed silica [42,152], nano-silica generated by the sol–gel method [93]. Silica has a silanol group on its surface, capable of interacting by hydrogen-bonding with the carbonyl group of the soft segments and urethane groups of the hard segment of PU [123]. Besides, the nano-silica surface can be functionalized with specific agents to prevent agglomeration and ensure stable covalent bonds between phases. Among these agents, it can be mentioned γ-trimethoxysilylpropyl methacrylate (TMSPM) [99,125,147], γ-methacryloxypropyltrimethoxysilane (MEMO) [87,89,93,162], PDMS [120], allyl isocyanate [42], poly (ethylene glycol) monomethyl ether methacrylate (PEGMA) [57], tetraethoxysilane (TEOS), and 3-glycidyloxypropyltrimethoxysilane (GLYMO) [108]. Furthermore, these coupling agents function effectively as a multifunctional crosslinker and can accelerate the curing speed of UV-WPU coatings [42,87,93].

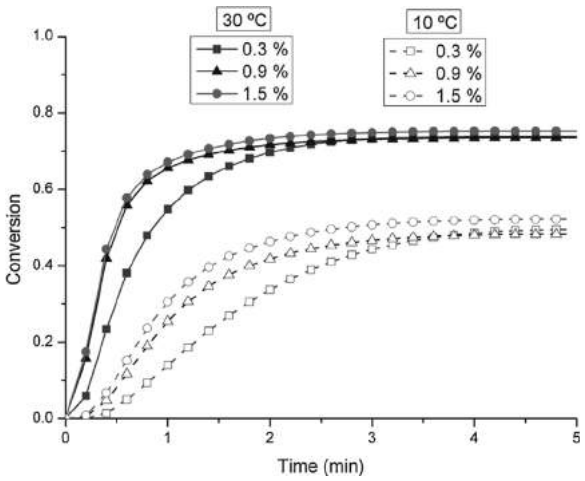

Fig. 9. Curing conversion of UV-WPU sample at 10 and 30 °C, using different photoinitiator amounts [32]. Reproduced with permission from Ref. 32, Llorente O, et al. (2016) Prog Org Coat 99:437–442. Copyright © 2016 Elsevier B.V.

The addition of functionalized silica to the UV-WPU chains contributed to improving the mechanical and thermal properties of the materials. The initial thermal decomposition temperature of the UV-WPU, especially that of the hard phase, gradually increased with the incorporation of growing levels of silica to the segmented PU [62,87–89,99,103,150]. The modified silica increases the prepolymer solution viscosity and, consequently, the particle size of the dispersion compared to unmodified silica [51,62,88,99,120,150].

Other fillers used are pigments. Pigments and nanoparticles with high UV light are harmful to photopolymerization due to the inhibition of free radicals that lead to binder polymerization, thus decreasing the curing degree in pigmented films [102,163]. Particles such as carbon black (CB) tend to agglomerate in dispersions and present a higher UV-light absorbency than other pigments, which causes the photoinitiator efficiency to decrease and the unsaturation conversions C = C of UV-WPU to be impaired [102]. On the other hand, zinc oxide (ZnO) nanoparticles have been used as an alternative to organic photoinitiators. ZnO reacts with water under UV irradiation to form hydrogen peroxide, and then active free radicals are generated to initiate the vinyl monomers photopolymerization [164]. An amount of 0.25 % wt.% ZnO showed a photoinitiation efficiency equivalent to 3–5 wt% of 2-hydroxyl-2-methyl-1-phenyl-1-propanone (Darocur 1173) [115,116]. However, the efficiency of this inorganic photoinitiator is limited to the presence of water. All the nanoparticles mentioned before must be added to UV-WPU systems in an ideal concentration. Above which, they can cause aggregation and heterogeneous distribution in the nanocomposite, compromising the properties of hardness, gel content, and mechanical resistance [45,70,76,108,135], as shown in Fig. 7. Naturally, it must be mentioned that introducing inorganic fillers into the resin matrix will roughen the surface of coatings.

3.5. *Effect of ionic groups content*

The production of water-based polyurethanes is related to incorporating a high number of hydrophilic groups in the polymer backbone, which enable solubility in water. For this, it is necessary to add hydrophilic chain extenders and blocked amine-containing ionic groups (such as dimethylol propionic acid with carboxyl groups), that react with the prepolymer. Non-ionic UV-WPU can be prepared similarly when the ionic center is replaced by a lateral or terminal hydrophilic ether chain [96,148]. Most commercial UV-WPU dispersions are only anionically stabilized with a dihydroxycarboxylic compound, such as, for example, DMPA and DMBA [38]. Although hydrophilic groups are essential for ionic dispersion, they retard drying and reduce hydrolytic stability [52,

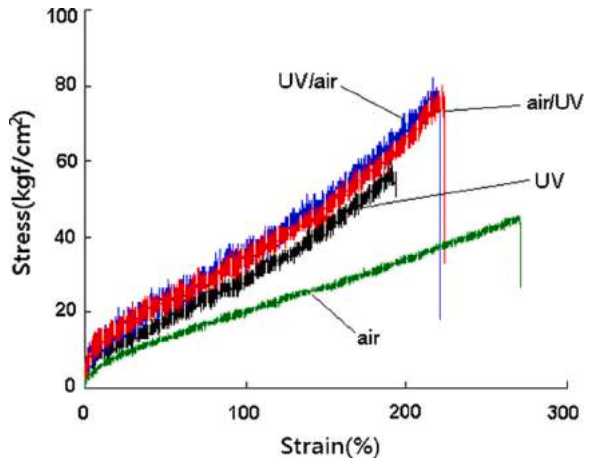

Fig. 10. Stress-strain curves of UV-WPU coatings prepared using different curing processes [138]. Reproduced with permission from Ref. 138, Chang, et al (2013) Prog Org Coat 76(7-8):1024–1031. Copyright © 2013 Elsevier B.V.

68,84,126]. Therefore, it is essential to minimize the emulsifier's content as much as possible while maintaining a stable dispersion. The emulsifier's ideal amount will depend on the original PU content, phase inversion temperature, and solvent affinity for water. In general, the amount of emulsifier is around 4 wt.% (based on the total solids content). When the hydrophilic group content (−COOH) in the UV-WPU resin is too low, it cannot be emulsified entirely, becoming unstable and partially condensing into blocks [80,95]. The increase in the amount of DMPA causes a reduction in the particle diameter, due to the higher density of ionic groups and the stabilization mechanism of ionomer dispersions [11,32,84,106]. As more carboxyl groups are incorporated into the UV-WPU structure, some characteristics such as adhesion, gloss, impact strength, and flexibility vary slightly, whereas the pendulum's hardness increases substantially. This can be attributed to more significant interchain interaction through coulombic forces and hydrogen bonding, derived from a higher DMPA content incorporation in the rigid segment [92].

The location of the ionic group and main backbone flexibility also affect the particle size. For example, the dispersion containing ionic groups in the soft segment has a much smaller particle size and higher viscosity than those containing ionic groups in the hard segment. This is because ionic groups can easily tailor the surface during dispersion owing to the easier change conformation in soft segments [24,33,50,61]. At the particle – water interface, a double layer is formed by the dissociation of ionic groups. The layer binds to UV-WPU chemically, and the counterion migrates into the water phase around the particle. The interference formed between electric double layers of different particles causes the repulsion between them, contributing to the dispersion stabilization. Adding an inert electrolyte to the ionomer dispersion reduces the range of bilayer repulsion and induces coagulation by providing additional ions at the water phase [11,34,92,126]. Viscosity is a property strongly dependent on the size and conformation of the chains. As the ionic groups in the polymer backbone increase, the mutual repulsion of similar charges causes the chain to expand, resulting in a viscosity increase of the UV-WPU dispersion. Furthermore, interchain associations resulting from hydrogen bonding between urethane and/or ureylene groups make the chains assume a more expanded conformation, which also contributes to the increase in viscosity. However, the intrachain hydrogen interactions formed can favor obtaining compact aggregates of UV-WPU ionomers, thus reducing viscosity. Therefore, the viscosity of the UV-WPU dispersion will be a consequence of the competition between these two phenomena [92].

Some authors have demonstrated that the amount of carboxylic acid introduced into the PU chain to make it water-dispersible may affect the curing kinetics by acting on the viscoelastic properties [101,165]. It was observed that the final conversion decreased as the acid content was increased. An increase in DMBA content from 4 wt.% to 8 wt.% caused the gel content to increase from 81.5%–88.8% and the water absorption decreased from 32.1 wt.% to 28.5 wt.%. This occurs due to the formation of chain entanglement, hydrogen bonding, and Coulomb interaction in the hard segments. The intermolecular interactions are enhanced, resulting in increased gel content and water resistance. In addition, denser films can be formed due to a decrease in particle size. However, when DMBA content is greater than 8 wt.% both the gel content and the water-resistance decrease. The excessive increase in intermolecular interactions amount restricts the molecular movement within the cured film and the reduction in the curing degree directly reflects in the reduction of the gel content and water resistance. Comparing the effects of DMBA and DMPA emulsifiers, Kim et al. [50] observed that a dispersion containing much finer particles was obtained in the presence of DMBA. Because the DMBA has a pendant alkyl group larger than DMPA, it is believed to have caused a more significant steric hindrance to the attack of carboxylic groups by isocyanate groups, leaving more carboxylic groups available for subsequent ionization.

During the first and second stages of UV-WPU formation, it is common to use a solvent to viscosity reduce the reaction medium. The addition of acetone, for example, results in a decrease of the viscosity medium, and also self-assembly of isocyanate-terminated prepolymer chains. Hard and soft segments are randomly located while dissolved in acetone. The solvents acetone and MEK are very suitable for controlling the viscosity during the chain extension step. In addition to being inert in the PU synthesis and non-reactive to isocyanates, they are miscible in water and easily removed by distillation due to their low boiling points (50–80 °C). An additional advantage of acetone is that it reduces the high reactivity of amine-based chain extenders with isocyanates through the reversible formation of ketamine [10].

3.6. *Effect of the neutralization degree*

The alkaline compound necessary to neutralize the carboxylic acid groups and obtain a stable aqueous dispersion plays a fundamental role in both the polymerization kinetics and the hydrophilic character of the UV-cured polymer [161]. The neutralization degree influences the particle mechanism formation. When the neutralization degree is below 70 %, the particles tend to aggregate and, therefore, do not stably disperse in water. On the other hand, increasing the neutralization degree causes a reduction in the WPU particle sizes. The higher number of dissociated carboxyl groups after neutralization contributes to stabilization. The viscosity of the dispersions also increases with the neutralization degree due to the increase in the hydrodynamic volume of the finer particles [95,126,128,130]. The increase in the neutralization degree also reduces the storage modulus, tensile strength, and glass transition, but contrarily, it increases the elongation at break. The neutralization probably results in a decrease of the local ordering of the hard segment regions, enabling the phase mixing due to the reduction of hydrogen bonding degree. This means that some C═O groups previously bonded to the NH of the urethane groups may be switched to bond with $^{+}NR_3H$ (TEA). It seems that TEA works as a plasticizer [127]. As shown in Table 1, TEA is the most used agent to neutralize carboxylic groups and to produce ionic centers to stabilize the polymer particle in water.

Feng et al. [116] evaluated the effect of different neutralization degrees on the gel content of UV-WPUs. The gel content gradually decreases as the neutralization degree is increased to 100 %. When the neutralization degree is 75 %, the gel content is 90.4 %. For neutralization degrees higher than 75 %, lower gelation rates were observed, which was related to a high content of TEA, and consequently, of active radicals at a short period during UV-curing. As a result, the UV-WPU was quickly UV-cured, leading to a viscous film and the cage effect that affects the subsequent UV-curing process. The increase in the neutralization degree caused a gradual increase in the film's hardness and a progressive reduction in water resistance. However, considering the

overall product's properties, UV-WPU dispersions and UV-cured films had the best performances when the neutralization degree was 100 %.

3.7. Dispersion process

The next step to neutralize the acid groups formed involves dispersing the WPU in water. In polar solvents, such as acetone, the PU ionomer solution spontaneously disperses when water is added. The transformation of an organic solution into an aqueous dispersion takes place in several steps. According to Dieterich [166], the initial addition of water leads to a sharp drop in viscosity due to the decrease in ionic bonding. The ionic interaction formed by the ionic center's neutralization is a reversible process, and water reduces these links between the centers and the molecular chains. As more water is added, the hydrophobic chain segment decreases due to the reduction of acetone concentration, and the hydrophobic-induced interaction by the hydrophobic segment increases its viscosity. Further addition of water leads to turbidity and the formation of a dispersed phase, followed by rearrangement to microspheres in which ions are formed superficially in the aggregate particles, resulting in reducing the viscosity [34]. As a result, PU nanoparticles self-assemble into a core-shell structure, where soft hydrophobic segments are surrounded by rigid hydrophilic segments [10]. Since most macromolecular chains are of great length with infinitesimally small cross profile, they curl to form a ball of string morphology [155]. Finally, the solvent used in the synthesis (usually acetone) is removed and a stable suspension, with a zeta potential of -40 to −65 mV, and a particle size of 10–300 nm is obtained. Typically, the finished urethane dispersion has a pH 7–8 and a solids content of 25–40 wt.% [21,32,33]. These dispersions remained stable without any change after 6 months of storage at room temperature [54,106,137,143].

Asif et al. [126] used deionized water, butyl alcohol, and methyl alcohol as dispersion mediums to investigate the effects of their dielectric constants on particle size with a 100 % neutralization degree. The average particle sizes increased as the dielectric constants decreased. The particle size in the different dispersion media followed the order of water < methanol < butanol. The higher the dielectric constant of the dispersion medium, the more significant is the dissociation of carboxyl groups. The concentration of dissociated groups mostly governs the average particle size; thus, higher dissociation is possible in high dielectric constant media (e.g., water).

For these formulations to be applied, formulators in coating industries always balance the viscosity, curing speed, and final properties for a given UV formulation. It is crucial to measure the viscosity of the dispersions as a function of the solids content since, for aqueous UV-curable resins, the water must be evaporated before photo-irradiation. Thus, a higher solid content with the same viscosity is beneficial in terms of energy efficiency.

In WPU dispersions, it is possible to obtain the ideal viscosity for the application, because the viscosity of dispersions is generally independent of the molecular weight of the polymer, it will depend on the particles size and the amount of solids present in the dispersion [126,127,167]. The rheological behavior of WPU dispersions belongs to pseudoplastic fluids [11,82,92,130,145]. A pseudoplastic and thixotropic behavior is interesting for coating applications, especially for spraying. When the coatings are sprayed from the spray-head at a high velocity, the greater shear rate reduces the apparent viscosity of the coatings. Coatings with lower viscosity (or good fluidity) are uniformly dispersed into fine spraying, giving a shiny and generous coat. During storage, the high viscosity of the coatings facilitates transportation efficiency and economic benefit [92].

3.8. Influence of the photoinitiator

The photoinitiator is extremely important in UV-radiation curing as it controls both the initiation rate and, the penetration of the incident light (cure depth). For water-based systems, the photoinitiator must be uniformly distributed in the film after the drying stage. For most photoinitiators, this can be achieved only by incorporating it into the WPU resin before the dispersion in water. The photoinitiator molecules will remain in the micelles until their coalescence by water removal, being then randomly distributed in the dry coating. So, the compatibility between the photoinitiator and WPU dispersions is required to properly cure the films [66,92,165]. The photoinitiator choice depends directly on its solubility in the medium, compatibility with resins, and, of course, the matching between its absorption peak and the waveband of the radiation source [32]. The photoinitiator will form active free radicals after energy absorption in the ultraviolet region, causing the additional polymerization of C═C bonds in monomers or oligomers. Fig. 8 shows several photoinitiators' influence on a WPU coating [165].

Some photoinitiators, such as hydroxyphenyl ketones (Irgacure 2959 and Darocur 1173), are partially soluble in water and can be incorporated into the aqueous dispersion to a certain concentration (1–5 wt.%) [68,165]. Fast and extensive curing can be achieved by using 4 wt.% of Darocur 1173. This photoinitiator appears to be particularly well suited when low temperatures are required for the drying and curing processes (~55 °C). For faster drying steps, under higher temperatures, this liquid photoinitiator is partially lost, and, in this case, solid hydroxyphenyl ketone (Irgacure 2959) is used, which has a higher thermal resistance. Masson et al. [165] confirmed that the photoinitiator content of the sample based on Irgacure 2959 remained essentially constant upon heating at 80 °C up to 1 h.

Another critical factor is that the amount of photoinitiator affects the final properties of the UV-WPU. Generally, the best properties are obtained with 3–4 wt% of the photoinitiator concerning the solids content [73,118,167]. The relationship between photoinitiator concentration and curing rate can be expressed by the general free radical polymerization rate Eq. (1) [91]:

$$R_P = k_p(fk_d/k_t)^{0.5}[M][I]^{0.5} \quad (1)$$

where R_P represents polymerization rate, *[M]* is the monomer concentration, *[I]* represents the photoinitiator concentration, k_d is the disproportionation termination rate constant of the termination reaction, and k_t represents the rate constant of the termination reaction. According to this equation, the polymerization reaction rate is proportional to the square root of the photoinitiator content. Consequently, within a specific range of curing time and concentration, the higher the photoinitiator concentration, the higher the crosslinking degree. However, as the photoinitiator content is above 5 wt.%, the C = C conversion is slightly reduced with a further increase of the photoinitiator. According to Lambert-Beer law, the light intensity behaves like a decreasing exponential as a function of the photoinitiator content increase [91].

The higher the photoinitiator content, the higher the amount of UV light absorbed, reflected, or scattered. This will not only reduce the radiation intensity distinctly but also generate abundant active free radicals on the UV-WPU film surface, leading to its rapid curing of C═C bonds. Meanwhile, the network structure reticulated on the film's surface can hinder the incidence of UV light, which reduces the absorption of this radiation by the bottom layer of UV-WPU materials. As a result, the gel content decreases slightly as the photoinitiator is in excess [66,91,101]. Also, the high concentration of photoinitiator will produce an excess of free radicals, which can easily combine with each other, interrupting the chain growth and decreasing the curing rate [22,86,111]. While the excess of photoinitiator leads to high cost, the insufficient amount of it generates a lower number of free radicals than necessary for the reaction, resulting in a low conversion of double bonds. Furthermore, excessive photoinitiator could lead to a high cost [22,111].

3.9. Curing process

Waterborne UV-curable coatings are crosslinked through a two-step process: water evaporation, and UV-curing. In any industrial application

of waterborne UV-curable coatings, the drying step will be the parameter that will control the curing line's speed since it is the slowest process [127,165]. In the water flash-off step, the physical entanglements occurred due to the approximation between the WPU nanoparticles to give a tack-free dried film [22]. The drying conditions (water drying rate and temperature) have significant effects on the surface properties and coatings' morphology. Insufficient or speedy drying can cause cracking, flaking, and bubble formation on the cured coating [24,168]. In the second UV-curing step, radicals formed by activated photoinitiators break the acrylate double bond resulting in a crosslinking structure [24,106]. Several factors determine the UV curing behavior, including the wavelength and intensity of radiation, the species and concentration of photoinitiator, reaction temperature, the viscosity of the acrylate formulation, the reactivity of functional groups, and others [22,33]. The difference in heat capacity between cured and non-cured materials, for example, decreased as a function of the photoinitiator concentration, which means that the crosslinking degree is higher for systems containing a lower photoinitiator content. This is because an increment in the photoinitiator concentration increases the termination reactions, leading to a reduction in the crosslinking degree [32].

The increase in temperature results in an increase in the reaction rate due to the polymer chains' higher segmental mobility, making the unsaturation sites more accessible for polymerization (Fig. 9) [32,142]. Masson et al. [165] demonstrated that a single pass under the UV lamp at a 20 m/min. speed was sufficient to polymerize 90 % of the acrylate double bonds when the sample temperature was 100 °C, compared to only 30 % at ambient. Based on these results, it is recommended to irradiate the hot sample immediately after performing the drying step, if acceptable for the substrate [32,161,165]. Faster and more complete polymerization can also be achieved by adding a diacrylate monomer to the dispersion to act as a reactive plasticizer. The maximum rate of polymerization shifts gradually for longer times as both photoinitiator content and temperature decrease. Thus, it is evident that at the end of the reaction, diffusion controls the reaction. The curing rate and the conversion increase with increasing the functionality of the end-capping groups, because coatings with higher functionality are easily activated and continue the reaction [24]. The exposure time to ultraviolet radiation, that is, the curing time also has a significant effect on the crosslinking of the material. When the curing time is short, the double bonds are not available entirely. When the curing time is prolonged, the curing degree remains unchanged [22].

Bai et al. [31] evaluated the effect of light intensity on the material's polymerization rate. The conversion of C═C bonds was low when the light intensity was 80 mW/cm^2 and increased as the light intensity increased until a specific maximum value. With the increase in light intensity, the number of radicals generated is higher, contributing to the inhibition of the negative effect of oxygen. However, when the light intensity is high enough, the radical-radical termination rate becomes faster than that of chain propagation, so the conversion is reversed or, at least, kept constant.

In general, the polymerization rate profiles of UV-curable prepolymers exhibit several typical features, which are autodeceleration, structural heterogeneity, and unequal functional group reactivity. During curing, the initial portions of curves involve a rapid increase in rates, while the second phases of polymerization involve a less fast increase and have generally been referred to as autoacceleration, that is, the polymerization rate increases despite the consumption of prepolymers. During autoacceleration, the mobility of radicals decreases dramatically, which leads to a reduction in the termination rate, as this step becomes controlled by diffusion. Finally, the polymerization reaction reaches a maximum rate and then begins to decrease. In this region (called autodeceleration) the vitrification crosslinking restricts and eventually stops the propagation. In these polymers, the bulk mobility of radicals is severely hindered, leading to a diffusion-limited termination mechanism [127]. According to Jansen et al. [169], acrylated prepolymers capable of hydrogen bonding exhibited 3–6 times higher polymerization rates than their non-hydrogen bonding counterparts.

Dual curing systems (UV/air and air/UV) have also been explored [138,139]. Such systems exhibited higher hardness than both coatings cured only by UV radiation, as can be seen in Fig. 10. In the structure of the dual-curing coating films, it was possible to detect the occurrence of both curing mechanisms: bulk free-radical polymerization and oxygen-dependent oxidation polymerization. The authors [138,139] stated that air-drying results in the formation of a skin layer with a higher crosslinking density. In air/UV dual-cured coatings, the initial air-drying to form a layer with a high crosslinking density acted as a barrier for the diffusion of oxygen to the inner layer of the film. This process was followed by rapid UV post-curing, which was the primary curing mechanism at the inner layer. The inner layer comprised more unsaturated double bonds, and a higher crosslinking density was therefore obtained after UV post-curing.

3.10. Applications

Waterborne UV-curable coatings have the performance and environmental requirements necessary for industrial applications as substrate protectors, such as wood, metal, automotive parts, synthetic leather, fabrics, and paper [43,91,110,138,153,163,165]. They can also be applied in the form of ink for flexographic printing packaging materials, magazines, and miscellaneous pieces of printing sectors [93]. For outdoor applications, these coatings may require light stabilizers, mainly UV absorbers, and HALS radical scavengers, to improve their weathering resistance and ensure efficient protection of the organic substrate against sunlight [153]. Mao et al. [91] applied UV-WPUs to coat cotton fabrics and noted that they have outstanding stability to UV light, although the color of the coated cotton fabrics turned slightly dim with prolonged UV curing time. The color fastness of the UV-WPUs-coated cotton fabrics can be improved to 4–5 grade with increasing the UV radiation and C = C content. Consequently, the UV-curable polymeric dyes with higher functionality are impressive when applied in textiles and other fields. The simple mixture of castor oil-based cationic WPU and acryloyl chloride modified lysozyme, followed by UV-curing, provided the coatings antibacterial properties [134]. Compared to thermally curable coatings, UV-curing technology is considered environmentally friendly, since the formulations release minimal amounts of VOCs and use less energy. Although the UV-curing process has been thoroughly investigated, as well as the resulting crosslinked polymers' properties, there is little information about the weathering resistance of waterborne UV-cured coatings.

The application of UV-cured polymer coatings is limited to flat objects with small and simple shapes, such as tabletops, doors, and wooden panels. The coating of a substrate with a complex configuration may result in shadow zones unreached by the UV radiation, which would lead to its incomplete curing. Besides that, pieces of thick layers could have their internal layers curing compromised, due to the limited light penetration. The oxygen inhibition resulting from molecular oxygen scavenging radicals is a significant limitation as it reduces the overall efficiency of UV-curable coatings. Other limitations can be detected for conventional UV-cured coatings, like non-uniform crosslinked films, and high internal stress.

Different methods have been developed to avoid the harmful effect of oxygen inhibition. These methods comprise purging inert gases, providing physical barriers, increasing light intensities [170], and photoinitiators content, adopting dual-curing hybrid photopolymerization [53,138], and adding hydrogen-donating chemicals such as tertiary amine [171] or thiol [149], which consume oxygen during curing. Thiol–ene photocurable reaction, also known as click reaction, has been used in conventional and waterborne radiation-curable coatings, due to its lower oxygen inhibition, uniform curing, and low-stress development.

Organic coatings or paints give an aesthetic appearance and protect against corrosion. The aesthetic properties of coatings, such as color and

brightness, can be manipulated as desired, but they must be committed to preserving the surface against environmental influences, including moisture, radiation, biological deterioration, or damages from mechanical and chemical origin. This refers to both interior and exterior applications. Typical corrosion-resistant coatings protect metallic surfaces mainly by two mechanisms: acting as a physical barrier to isolate the substrate from a corrosive environment, or containing inhibiting agents (usually pigments) in their composition, which interact with a vehicle component and inhibit corrosion [1]. There must be a viscous flow of polymer chains near the coating surface so that it tacks to the substrate. In terms of tack and chain mobility, UV-WPU coatings with cyclic structures are less efficient than those with linear architectures and similar molar masses. Tack free before curing is an essential property for a resilient flooring application, for example, since its coated surface can be embossed without sticking to the embossing roll [40,46,50].

4. Conclusions and perspectives

The current review presents the recent development in UV-curable waterborne polyurethane (WPU) materials, concerning the formulation components' effects on the film's final properties. This paper reports on monomer, photoinitiators, chain extender, and reactive diluents characteristic of UV-curable WPUs, and the main applications associated with intelligent materials developed from them. In recent years, the appeal for more environmentally friendly and high-performance coatings at a reasonable cost has resulted in many UV-WPU production processes being improved. The consequence was the emergence of innumerable UV-WPU possible formulations, from which specific material properties and applications could be obtained. Interestingly, few reports on these systems are available to the scientific community, especially for researchers interested in developing innovative formulations based on existing ones. In this context, this literature analysis aimed to enlighten the interested parties about the main characteristics of these coatings and which formulations have already been tested, contributing to a conscious system choice for a given application. It is now clearer which UV-WPU composition has been most used in art and the main challenges faced by scientists.

From the studies reported in Table 1 of this paper, researchers will find new applications for the polymer systems that have already been tested. It will also be possible to optimize the limitations reported by other authors and have insights for new materials. With a deeper understanding of these coatings' chemistry at the molecular level, it will be possible to create specific micro and nanosystems with adjustable properties. The proper selection of monomers and nanofillers and functionalization types is crucial to control these materials' physicochemical properties. Also, the election of additives and processing conditions can significantly change the properties of UW-WPUs. Therefore, understanding this correlation is essential for a more intelligent selection of synthesis parameters and precursors and, consequently, for obtaining photocurable films with specific properties. UV-cure technology will grow within coating technology as the properties of the coatings improve. While radical-induced polymerizations resulting from UV irradiation can be fast, the need to evaporate water from the coating can slow down manufacturing line speeds. However, as formulations improve and solids levels increase, the waterborne coatings become an increasingly attractive option. These coatings' dual-cure nature allows for tuned crosslink densities and the possibility of higher final coating crosslink densities at lower initial viscosity than obtained with other coating technologies. The appeal for sustainable and green products and processes, the substitution of petroleum derivatives for renewable energy sources, and the advent of biodegradable and biocompatible polymers will result in the need to formulate advanced materials, particularly in biopharmaceutical and biomedical areas. Hybrids from various organic and inorganic materials, particularly those formulated with sustainable raw materials (starch, gelatin, cellulose, etc.), can impart biodegradable properties and broaden the UV-WPU application spectrum. The addition of fillers carrying multiple −OH groups to the WPU matrix also provides multifunctional cross-links that further increase the new formulations' strength [172–174]. Cross-linking WPUs containing siloxane bonding, for example, have shown a reinforcement effect on thermal and surface properties of UV-WPU systems [175,176]. Combining these approaches has shown to be an efficient technology for improving the performance of WPU systems [177]. UV-curable WPU materials are currently applied as antibacterial, antistatic, flame retardant, and antifog coatings to protect or beautify the wood, plastic, metal, and paper surface through the appropriate selection of nanoparticles, additives, monomers, chain extenders, reactive diluents, among others. There is, however, an enduring need to refine these systems to improve their properties so that their potential application areas are extended. Definitely, these UV-curable WPU coatings will bring appealing benefits to the polymer field, especially due to their production technology, which besides being water-based with no solvents, also uses a fast, low energy, and cleaner curing source. In addition to being green materials, these coatings still present flexibility, durability, chemical resistance, and high adhesive force. Therefore, they end up being more advantageous in comparison with conventional thermosetting solvent resins.

Declaration of Competing Interest

The authors declare that they have no known competing financial interests or personal relationships that could have appeared to influence the work reported in this paper.

Acknowledgments

The authors acknowledge Brazilian Agency *Coordenação de Aperfeiçoamento de Pessoal de Nível Superior* (CAPES, Brazil) – (Finance Code 001), Conselho Nacional de Desenvolvimento Científico e Tecnológico (CNPq, Brazil) and Fundação de Amparo à Pesquisa do Estado do Rio Grande do Sul (FAPERGS, Brazil) for scholarships and research financial (grants: 19/2551-0001843-6 and 306086/2018-2).

Appendix A. Supplementary data

Supplementary material related to this article can be found, in the online version, at doi:https://doi.org/10.1016/j.porgcoat.2021.106156.

References

[1] D.K. Chattopadhyay, K.V.S.N. Raju, Structural engineering of polyurethane coatings for high performance applications, Prog. Polym. Sci. 32 (2007) 352–418, https://doi.org/10.1016/j.progpolymsci.2006.05.003.
[2] M.S. Kathalewar, P.B. Joshi, A.S. Sabnis, V.C. Malshe, Non-isocyanate polyurethanes: from chemistry to applications, RSC Adv. 3 (2013) 4110–4129, https://doi.org/10.1039/c2ra21938g.
[3] A. Santamaria-Echart, A. Arbelaiz, A. Saralegi, B. Fernández-d'Arlas, A. Eceiza, M.A. Corcuera, Relationship between reagents molar ratio and dispersion stability and film properties of waterborne polyurethanes, Colloids Surf. A Physicochem. Eng. Asp. 482 (2015) 554–561, https://doi.org/10.1016/j.colsurfa.2015.07.012.
[4] L.D. Agnol, H.L. Ceratti, D. Favero, S.P. Rempel, Ld.S.A. Schiavo, J.R. Ernzen, F.T. G. Dias, O. Bianchi, Transurethanization reaction as an alternative for melt modification of polyamide 6, J. Polym. Res. 26 (2019) 112, https://doi.org/10.1007/s10965-019-1787-4.
[5] G.B. Kim, J. Guo, J. Hu, D. Shan, J. Yang, Novel applications of urethane/urea chemistry in the field of biomaterials. Advances in Polyurethane Biomaterials, Woodhead Publishing, 2016, pp. 115–147, https://doi.org/10.1016/B978-0-08-100614-6.00004-4.
[6] T. Zhang, W. Wu, X. Wang, Y. Mu, Effect of average functionality on properties of UV-curable waterborne polyurethane-acrylate, Prog. Org. Coat. 68 (2010) 201–207, https://doi.org/10.1016/j.porgcoat.2010.02.004.
[7] Z.H. Fang, J.J. Shang, Y.X. Huang, J. Wang, D.Q. Li, Z.Y. Liu, Preparation and characterization of the heat-resistant UV curable waterborne polyurethane coating modified by bisphenol A, Express Polym. Lett. 4 (2010) 704–711, https://doi.org/10.3144/expresspolymlett.2010.85.

[8] V. García-Pacios, V. Costa, M. Colera, J.M. Martín-Martínez, Waterborne polyurethane dispersions obtained with polycarbonate of hexanediol intended for use as coatings, Prog. Org. Coat. 71 (2011) 136–146, https://doi.org/10.1016/j.porgcoat.2011.01.006.

[9] J. Wang, H. Zhang, Y. Miao, L. Qiao, X. Wang, F. Wang, UV-curable waterborne polyurethane from CO_2-polyol with high hydrolysis resistance, Polymer 100 (2016) 219–226, https://doi.org/10.1016/j.polymer.2016.08.039.

[10] X. Zhou, C. Fang, W. Lei, J. Du, T. Huang, Y. Li, Y. Cheng, Various nanoparticle morphologies and surface properties of waterborne polyurethane controlled by water, Sci. Rep. 6 (2016) 34574, https://doi.org/10.1038/srep34574.

[11] A. Asif, W. Shi, X. Shen, K. Nie, Physical and thermal properties of UV curable waterborne polyurethane dispersions incorporating hyperbranched aliphatic polyester of varying generation number, Polymer 46 (2005) 11066–11078, https://doi.org/10.1016/j.polymer.2005.09.046.

[12] J. Aizpurua, L. Martin, M. Fernández, A. González, L. Irusta, Recyclable, remendable and healing polyurethane/acrylic coatings from UV curable waterborne dispersions containing Diels-Alder moieties, Prog. Org. Coat. 139 (2020), 105460, https://doi.org/10.1016/j.porgcoat.2019.105460.

[13] Y. Xia, R.C. Larock, Castor-oil-based waterborne polyurethane dispersions cured with an Aziridine-based crosslinker, Macromol. Mater. Eng. 296 (2011) 703–709, https://doi.org/10.1002/mame.201000431.

[14] J.W. Gooch, H. Dong, F.J. Schork, Waterborne oil-modified polyurethane coatings via hybrid miniemulsion polymerization, J. Appl. Polym. Sci. 76 (2000) 105–114, https://doi.org/10.1002/(sici)1097-4628(20000404)76:1<105::Aid-app14>3.0.Co;2-8.

[15] S. Turri, M. Levi, T. Trombetta, Waterborne anionomeric polyurethane-ureas from functionalized fluoropolyethers, J. Appl. Polym. Sci. 93 (2004) 136–144, https://doi.org/10.1002/app.20441.

[16] J. Yoon Jang, Y. Kuk Jhon, I. Woo Cheong, J. Hyun Kim, Effect of process variables on molecular weight and mechanical properties of water-based polyurethane dispersion, Colloids Surf. A Physicochem. Eng. Asp. 196 (2002) 135–143, https://doi.org/10.1016/s0927-7757(01)00857-3.

[17] D.-Y. Xie, F. Song, M. Zhang, X.-L. Wang, Y.-Z. Wang, Roles of soft segment length in structure and property of soy protein isolate/waterborne polyurethane blend films, Ind. Eng. Chem. Res. 55 (2016) 1229–1235, https://doi.org/10.1021/acs.iecr.5b04185.

[18] Y. Zhang, L. Shao, B. Liu, F. Wang, Y. Wang, Effect of molecular weight of liquid polysulfide on water and organic solvent resistances of waterborne polyurethane/polysulfide copolymer, Prog. Org. Coat. 112 (2017) 219–224, https://doi.org/10.1016/j.porgcoat.2017.07.010.

[19] F. Yu, L. Cao, Z. Meng, N. Lin, X.Y. Liu, Crosslinked waterborne polyurethane with high waterproof performance, Polym. Chem. 7 (2016) 3913–3922, https://doi.org/10.1039/c6py00350h.

[20] T.J. Lee, S.H. Kwon, B.K. Kim, Biodegradable sol-gel coatings of waterborne polyurethane/gelatin chemical hybrids, Prog. Org. Coat. 77 (2014) 1111–1116, https://doi.org/10.1016/j.porgcoat.2014.03.011.

[21] Z. Niu, F. Bian, Synthesis and characterization of multiple cross-linking UV-curable waterborne polyurethane dispersions, Iran Polym. J. 21 (2012) 221–228, https://doi.org/10.1007/s13726-012-0021-6.

[22] H. Xu, F. Qiu, Y. Wang, W. Wu, D. Yang, Q. Guo, UV-curable waterborne polyurethane-acrylate: preparation, characterization and properties, Prog. Org. Coat. 73 (2012) 47–53, https://doi.org/10.1016/j.porgcoat.2011.08.019.

[23] Z. Niu, X. Zhang, J. Dai, H. Zhang, Investigation of ultraviolet curable waterborne polyurethane acrylate dispersion based on hydroxyl-terminated polybutadiene, Front. Chem. China 2 (2007) 151–155, https://doi.org/10.1007/s11458-007-0031-7.

[24] H.-D. Hwang, C.-H. Park, J.-I. Moon, H.-J. Kim, T. Masubuchi, UV-curing behavior and physical properties of waterborne UV-curable polycarbonate-based polyurethane dispersion, Prog. Org. Coat. 72 (2011) 663–675, https://doi.org/10.1016/j.porgcoat.2011.07.009.

[25] J. Fu, L. Wang, H. Yu, M. Haroon, F. Haq, W. Shi, B. Wu, L. Wang, Research progress of UV-curable polyurethane acrylate-based hardening coatings, Prog. Org. Coat. 131 (2019) 82–99, https://doi.org/10.1016/j.porgcoat.2019.01.061.

[26] Y. Deng, C. Zhou, Q. Zhang, M. Zhang, H. Zhang, Structure and performance of waterborne polyurethane-acrylate composite emulsions for industrial coatings: effect of preparation methods, Colloid Polym. Sci. 298 (2019) 139–149, https://doi.org/10.1007/s00396-019-04583-6.

[27] S.L. Chai, M.M. Jin, H.M. Tan, Comparative study between core-shell and interpenetrating network structure polyurethane/polyacrylate composite emulsions, Eur. Polym. J. 44 (2008) 3306–3313, https://doi.org/10.1016/j.eurpolymj.2008.07.038.

[28] C. Yang, V. Castelvetro, Y. Zhang, C. Hu, Facile hydrophobic modification of hybrid poly(urethane-urea)methacrylate aqueous dispersions and films through blending with novel waterborne fluorinated acrylic copolymers, Colloid Polym. Sci. 290 (2011) 491–506, https://doi.org/10.1007/s00396-011-2565-y.

[29] G.A. Alvarez, M. Fuensanta, V.H. Orozco, L.F. Giraldo, J.M. Martín-Martínez, Hybrid waterborne polyurethane/acrylate dispersion synthesized with bisphenol A-glicidylmethacrylate (Bis-GMA) grafting agent, Prog. Org. Coat. 118 (2018) 30–39, https://doi.org/10.1016/j.porgcoat.2018.01.016.

[30] I. Barbara, M.-A. Dourges, H. Deleuze, Preparation of porous polyurethanes by emulsion-templated step growth polymerization, Polymer 132 (2017) 243–251, https://doi.org/10.1016/j.polymer.2017.11.018.

[31] C.Y. Bai, X.Y. Zhang, J.B. Dai, W.H. Li, A new UV curable waterborne polyurethane: effect of C=C content on the film properties, Prog. Org. Coat. 55 (2006) 291–295, https://doi.org/10.1016/j.porgcoat.2005.12.002.

[32] O. Llorente, M.J. Fernández-Berridi, A. González, L. Irusta, Study of the crosslinking process of waterborne UV curable polyurethane acrylates, Prog. Org. Coat. 99 (2016) 437–442, https://doi.org/10.1016/j.porgcoat.2016.06.020.

[33] H.-D. Hwang, H.-J. Kim, Enhanced thermal and surface properties of waterborne UV-curable polycarbonate-based polyurethane (meth)acrylate dispersion by incorporation of polydimethylsiloxane, React. Funct. Polym. 71 (2011) 655–665, https://doi.org/10.1016/j.reactfunctpolym.2011.03.004.

[34] E.J. Shin, S.M. Choi, Advances in waterborne polyurethane-based biomaterials for biomedical applications, Adv. Exp. Med. Biol. 1077 (2018) 251–283, https://doi.org/10.1007/978-981-13-0947-2_14.

[35] D.B. Otts, L.A. Cueva-Parra, R.B. Pandey, M.W. Urban, Film formation from aqueous polyurethane dispersions of reactive hydrophobic and hydrophilic components; spectroscopic studies and Monte Carlo simulations, Langmuir 21 (2005) 4034–4042, https://doi.org/10.1021/la047564r.

[36] S.D. Maurya, S.K. Kurmvanshi, S. Mohanty, S.K. Nayak, A review on acrylate-terminated urethane oligomers and polymers: synthesis and applications, Polym. Technol. Eng. 57 (2017) 625–656, https://doi.org/10.1080/03602559.2017.1332764.

[37] Y. Ahmadi, S. Ahmad, Recent progress in the synthesis and property enhancement of waterborne polyurethane nanocomposites: promising and versatile macromolecules for advanced applications, Polym. Rev. 60 (2019) 226–266, https://doi.org/10.1080/15583724.2019.1673403.

[38] H. Honarkar, Waterborne polyurethanes: a review, J. Dispers. Sci. Technol. 39 (2017) 507–516, https://doi.org/10.1080/01932691.2017.1327818.

[39] X. Zhou, Y. Li, C. Fang, S. Li, Y. Cheng, W. Lei, X. Meng, Recent advances in synthesis of waterborne polyurethane and their application in water-based ink: a review, J. Mater. Sci. Technol. 31 (2015) 708–722, https://doi.org/10.1016/j.jmst.2015.03.002.

[40] B.U. Ahn, S.K. Lee, S.K. Lee, H.M. Jeong, B.K. Kim, High performance UV curable polyurethane dispersions by incorporating multifunctional extender, Prog. Org. Coat. 60 (2007) 17–23, https://doi.org/10.1016/j.porgcoat.2007.06.001.

[41] Y.D. Meng, H.W. Li, The structure and properties of UV-curable cationic waterborne polyurethane acrylate, Adv. Mat. Res. 1090 (2015) 31–37, https://doi.org/10.4028/www.scientific.net/AMR.1090.31.

[42] S.K. Lee, S.H. Yoon, I. Chung, A. Hartwig, B.K. Kim, Waterborne polyurethane nanocomposites having shape memory effects, J. Polym. Sci. A Polym. Chem. 49 (2011) 634–641, https://doi.org/10.1002/pola.24473.

[43] F. Deflorian, M. Fedel, A. DiGianni, R. Bongiovanni, S. Turri, Corrosion protection properties of new UV-curable waterborne urethane acrylic coatings, Corros. Eng. Sci. Techn. 43 (2008) 81–86, https://doi.org/10.1179/174327808x286194.

[44] C. Bai, X. Zhang, J. Dai, Synthesis and characterization of a new UV cross-linkable waterborne siloxane-polyurethane dispersion, J. Macromol. Sci. A. 44 (2007) 1203–1208, https://doi.org/10.1080/10601320701561163.

[45] G. Chen, S. Ouyang, Y. Deng, M. Chen, Y. Zhao, W. Zou, Q. Zhao, Improvement of self-cleaning waterborne polyurethane-acrylate with cationic TiO2/reduced graphene oxide, RSC Adv. 9 (2019) 18652–18662, https://doi.org/10.1039/c9ra03250a.

[46] B.U. Ahn, S.K. Lee, S.K. Lee, J.H. Park, B.K. Kim, UV curable polyurethane dispersions from polyisocyanate and organosilane, Prog. Org. Coat. 62 (2008) 258–264, https://doi.org/10.1016/j.porgcoat.2008.01.001.

[47] M.H. Lee, H.Y. Choi, K.Y. Jeong, J.W. Lee, T.W. Hwang, B.K. Kim, High performance UV cured polyurethane dispersion, Polym. Degrad. Stab. 92 (2007) 1677–1681, https://doi.org/10.1016/j.polymdegradstab.2007.06.006.

[48] M.H. Lee, M.K. Jang, B.K. Kim, Surface modification of high heat resistant UV cured polyurethane dispersions, Eur. Polym. J. 43 (2007) 4271–4278, https://doi.org/10.1016/j.eurpolymj.2007.07.044.

[49] H.Y. Choi, C.Y. Bae, B.K. Kim, Nanoclay reinforced UV curable waterborne polyurethane hybrids, Prog. Org. Coat. 68 (2010) 356–362, https://doi.org/10.1016/j.porgcoat.2010.03.015.

[50] B.K. Kim, B.U. Ahn, M.H. Lee, S.K. Lee, Design and properties of UV cured polyurethane dispersions, Prog. Org. Coat. 55 (2006) 194–200, https://doi.org/10.1016/j.porgcoat.2005.09.015.

[51] S. Zhang, Z. Chen, M. Guo, H. Bai, X. Liu, Synthesis and characterization of waterborne UV-curable polyurethane modified with side-chain triethoxysilane and colloidal silica, Colloids Surf. A Physicochem. Eng. Asp. 468 (2015) 1–9, https://doi.org/10.1016/j.colsurfa.2014.12.004.

[52] C.Y. Bai, X.Y. Zhang, J.B. Dai, C.Y. Zhang, Water resistance of the membranes for UV curable waterborne polyurethane dispersions, Prog. Org. Coat. 59 (2007) 331–336, https://doi.org/10.1016/j.porgcoat.2007.05.003.

[53] C. Bai, X. Zhang, J. Dai, Effect of the hard segment on the properties of UV curable waterborne blocked polyurethanes, J. Polym. Res. 15 (2007) 67–73, https://doi.org/10.1007/s10965-007-9144-4.

[54] C. Bai, X. Zhang, J. Dai, Synthesis and characterization of PDMS modified UV-curable waterborne polyurethane dispersions for soft tact layers, Prog. Org. Coat. 60 (2007) 63–68, https://doi.org/10.1016/j.porgcoat.2007.07.003.

[55] Y.B. Kim, H.K. Kim, J.K. Yoo, J.W. Hong, UV-curable polyurethane dispersion for cationic electrodeposition coating, Surf. Coat. Technol. 157 (2002) 40–46, https://doi.org/10.1016/s0257-8972(02)00133-0.

[56] H.-J. Yin, Z. Xiong, S.-J. Yan, Z.-M. Chen, Y.-Q. Xiong, W.-J. Xu, UV-curable hybrids of hyperbranched and linear polyurethane dispersions, J. Macromol. Sci. B 51 (2011) 209–223, https://doi.org/10.1080/00222348.2011.585315.

[57] S. Zhang, A. Yu, X. Song, X. Liu, Synthesis and characterization of waterborne UV-curable polyurethane nanocomposites based on the macromonomer surface modification of colloidal silica, Prog. Org. Coat. 76 (2013) 1032–1039, https://doi.org/10.1016/j.porgcoat.2013.02.019.

[58] Y. Wei, H. Xin, Effect of diisocyanates on the structure and properties of UV-curable polyurethane dispersions with nano-scale particles, e-Polymers 8 (2008) 169, https://doi.org/10.1515/epoly.2008.8.1.1926.
[59] S.H. Yoon, B.K. Kim, UV-curable water-borne polyurethane primers for aluminum and polycarbonate interfaces, Polym. Bull. 68 (2011) 529–539, https://doi.org/10.1007/s00289-011-0637-2.
[60] Z. Ge, C. Huang, C. Zhou, Y. Luo, Synthesis of a novel UV crosslinking waterborne siloxane–polyurethane, Prog. Org. Coat. 90 (2016) 304–308, https://doi.org/10.1016/j.porgcoat.2015.10.011.
[61] D.H. Jung, E.Y. Kim, Y.S. Kang, B.K. Kim, High solid and high performance UV cured waterborne polyurethanes, Colloids Surf. A Physicochem. Eng. Asp. 370 (2010) 58–63, https://doi.org/10.1016/j.colsurfa.2010.08.046.
[62] B.S. Kim, S.H. Park, B.K. Kim, Nanosilica-reinforced UV-cured polyurethane dispersion, Colloid Polym. Sci. 284 (2006) 1067–1072, https://doi.org/10.1007/s00396-006-1488-5.
[63] M. Zhang, Y.D. Meng, H.W. Li, H.W. Li, Curing behavior of the UV-curable cationic waterborne polyurethane acrylate adhesives, Mater. Sci. Environ. Eng. (2016) 507–515, https://doi.org/10.1142/9789813143401_0057.
[64] C. Shan, C. Ning, J. Lou, W. Xu, Y. Zhang, Design and preparation of UV-curable waterborne polyurethane based on novel fluorinated chain extender, Polym. Bull. (2020), https://doi.org/10.1007/s00289-020-03202-7.
[65] S. Zhang, J. Chen, D. Han, Y. Feng, C. Shen, C. Chang, Z. Song, J. Zhao, Effect of polyether soft segments on structure and properties of waterborne UV-curable polyurethane nanocomposites, J. Coat. Technol. Res. 12 (2015) 563–569, https://doi.org/10.1007/s11998-014-9654-z.
[66] E. Bakhshandeh, S. Bastani, M.R. Saeb, C. Croutxé-Barghorn, X. Allonas, High-performance water-based UV-curable soft systems with variable chain architecture for advanced coating applications, Prog. Org. Coat. 130 (2019) 99–113, https://doi.org/10.1016/j.porgcoat.2019.01.033.
[67] A. Matev, P. Velev, S. Ismail, M. Herzog, Preparing, properties and application of waterborne polyurethane-acrylate oligomer as a matrix in UV-cured fiberglasses, Bulg. Chem. Commun. 49 (2017) 174–180.
[68] Z.W. Liu, J.Y. He, W.J. Kang, X.D. Luo, Y.M. Ding, P.C. Xie, Study on the synthesis of waterborne UV curable polyurethane acrylate, Key Eng. Mater. 703 (2016) 256–260, https://doi.org/10.4028/www.scientific.net/KEM.703.256.
[69] Y.B. Jiu, X.M. Zeng, J.H. Ji, Y. Zhai, L.C. Wang, Properties of high solid content UV curable waterborne polyurethane dispersions with different C=C content, Adv. Mat. Res. 535–537 (2012) 1158–1162, https://doi.org/10.4028/www.scientific.net/AMR.535-537.1158.
[70] S. Chen, S. Zhang, Y. Li, G. Zhao, Synthesis and properties of novel UV-curable hyperbranched waterborne polyurethane/Fe3O4 nanocomposite films with excellent magnetic properties, RSC Adv. 5 (2015) 4355–4363, https://doi.org/10.1039/c4ra13683g.
[71] S. Chen, W. Wu, G. Zhao, T. Jin, T. Zhao, Fabrication and properties of superparamagnetic UV-curable nanocomposites based on covalently linked waterborne polyurethane/functionalized hollow Ni0.3Zn0.5Fe2O4 microspheres, RSC Adv. 5 (2015) 47788–47797, https://doi.org/10.1039/c5ra01708d.
[72] Z. Fang, M. Zhou, J. Zhong, Y. Qi, L. Li, Q. Dong, Preparation and properties of novel ultraviolet-cured waterborne polyurethanes, High. Perform. Polym. 25 (2013) 668–676, https://doi.org/10.1177/0954008313479983.
[73] L. Boton, J.M. Puguan, M. Latif, H. Kim, Synthesis and properties of quick-drying UV-curable hyperbranched waterborne polyurethane coating, Prog. Org. Coat. 125 (2018) 201–206, https://doi.org/10.1016/j.porgcoat.2018.09.017.
[74] T. Liu, X. Pan, Y. Wu, T. Zhang, Z. Zheng, X. Ding, Y. Peng, Synthesis and characterization of UV-curable waterborne polyurethane acrylate possessing perfluorooctanoate side-chains, J. Polym. Res. 19 (2012) 9741, https://doi.org/10.1007/s10965-011-9741-0.
[75] H. Liu, H. Zhang, C. Peng, S. Ren, C. Yuan, W. Luo, G. Chen, F. He, L. Dai, UV-curable waterborne polyurethane dispersions modified with a trimethoxysilane end-capping agent and edge-hydroxylated boron nitride, J. Coat. Technol. Res. 16 (2019) 1479–1492, https://doi.org/10.1007/s11998-019-00232-3.
[76] X. Wang, Y. Hu, L. Song, W. Xing, H. Lu, P. Lv, G. Jie, Effect of antimony doped tin oxide on behaviors of waterborne polyurethane acrylate nanocomposite coatings, Surf. Coat. Technol. 205 (2010) 1864–1869, https://doi.org/10.1016/j.surfcoat.2010.08.053.
[77] J. Tan, W. Liu, Z. Wang, Preparation and performance of waterborne UV-curable polyurethane containing long fluorinated side chains, J. Appl. Polym. Sci. 134 (2017) 44506, https://doi.org/10.1002/app.44506.
[78] H.A. Kim, B.K. Kim, Synthesis and properties of waterborne polyurethane/hydroxyapatite chemical hybrids, Prog. Org. Coat. 128 (2019) 69–74, https://doi.org/10.1016/j.porgcoat.2018.12.009.
[79] X. Wang, Y. Hu, L. Song, W. Xing, H. Lu, P. Lv, G. Jie, UV-curable waterborne polyurethane acrylate modified with octavinyl POSS for weatherable coating applications, J. Polym. Res. 18 (2010) 721–729, https://doi.org/10.1007/s10965-010-9468-3.
[80] J.Y. He, Y. Liu, L.C. He, Q. Wang, Research on the modification of waterborne UV-curable polyurethane acrylate, Adv. Mat. Res. 864–867 (2013) 698–701, https://doi.org/10.4028/www.scientific.net/AMR.864-867.698.
[81] A.C. Aznar, O.R. Pardini, J.I. Amalvy, Glossy topcoat exterior paint formulations using water-based polyurethane/acrylic hybrid binders, Prog. Org. Coat. 55 (2006) 43–49, https://doi.org/10.1016/j.porgcoat.2005.11.001.
[82] Q. Yong, B. Liao, J. Huang, Y. Guo, C. Liang, H. Pang, Preparation and characterization of a novel low gloss waterborne polyurethane resin, Surf. Coat. Technol. 341 (2018) 78–85, https://doi.org/10.1016/j.surfcoat.2018.01.012.
[83] S. Yao, J. Shi, X. Du, M. Lu, Y. Liu, L. Liang, M. Lu, Preparation, characterization and application of cyclodextrin-containing UV-curable waterborne polyurethane based on guest regulation, ChemistrySelect. 5 (2020) 2255–2262, https://doi.org/10.1002/slct.201904348.
[84] X.Q. Zhou, Y.M. Cao, J.L. Tian, Synthesis and properties of waterborne UV polyurethane, Adv. Mat. Res. 311–313 (2011) 1087–1092, https://doi.org/10.4028/www.scientific.net/AMR.311-313.1087.
[85] W.Y. Li, Y.M. Cao, X.Q. Zhou, Study on UV curable waterborne polyurethane modified by epoxy resin, Appl. Mech. Mater. 249–250 (2012) 842–848, https://doi.org/10.4028/www.scientific.net/AMM.249-250.842.
[86] R.X. Xu, G.X. Chen, Study on photopolymerization performance of waterborne UV cured ink, Adv. Mat. Res. 174 (2010) 401–404, https://doi.org/10.4028/www.scientific.net/AMR.174.401.
[87] C. Lv, L. Hu, Y. Yang, H. Li, C. Huang, X. Liu, Waterborne UV-curable polyurethane acrylate/silica nanocomposites for thermochromic coatings, RSC Adv. 5 (2015) 25730–25737, https://doi.org/10.1039/c5ra01687h.
[88] S. Zhang, RenLiu, J. Jiang, C. Yang, M. Chen, X. Liu, Facile synthesis of waterborne UV-curable polyurethane/silica nanocomposites and morphology, physical properties of its nanostructured films, Prog. Org. Coat. 70 (2011) 1–8, https://doi.org/10.1016/j.porgcoat.2010.09.005.
[89] S. Zhang, A. Yu, S. Liu, J. Zhao, J. Jiang, X. Liu, Effect of silica nanoparticles on structure and properties of waterborne UV-curable polyurethane nanocomposites, Polym. Bull. 68 (2011) 1469–1482, https://doi.org/10.1007/s00289-011-0689-3.
[90] X. Zhang, M. Zhu, W. Wang, D. Yu, Silver/waterborne polyurethane-acrylate's antibacterial coating on cotton fabric based on click reaction via ultraviolet radiation, Prog. Org. Coat. 120 (2018) 10–18, https://doi.org/10.1016/j.porgcoat.2018.03.004.
[91] H. Mao, S. Qiang, Y. Xu, C. Wang, Synthesis of polymeric dyes based on UV curable multifunctional waterborne polyurethane for textile coating, New J. Chem. 41 (2017) 619–627, https://doi.org/10.1039/c6nj03159e.
[92] J. Yang, Z. Wang, Z. Zeng, Y. Chen, Chain-extended polyurethane-acrylate ionomer for UV-curable waterborne coatings, J. Appl. Polym. Sci. 84 (2002) 1818–1831, https://doi.org/10.1002/app.10384.
[93] J. Zhang, H. Xu, L. Hu, Y. Yang, H. Li, C. Huang, X. Liu, Novel waterborne UV-curable hyperbranched polyurethane acrylate/silica with good printability and rheological properties applicable to flexographic ink, ACS Omega 2 (2017) 7546–7558, https://doi.org/10.1021/acsomega.7b00939.
[94] H. Liao, B. Zhang, L. Huang, D. Ma, Z. Jiao, Y. Xie, S. Tan, X. Cai, The utilization of carbon nitride to reinforce the mechanical and thermal properties of UV-curable waterborne polyurethane acrylate coatings, Prog. Org. Coat. 89 (2015) 35–41, https://doi.org/10.1016/j.porgcoat.2015.07.021.
[95] Y. Guo, C. Chen, F. Chu, Study on the preparation of waterborne UV-curable polyurethane acrylate, in: X.M.Y. Ouyang, L. Yang, Y. Ouyang (Eds.), Advanced Graphic Communications, Packaging Technology and Materials. Lecture Notes in Electrical Engineering, Springer, Singapore, 2016, https://doi.org/10.1007/978-981-10-0072-0_115.
[96] X. Zhu, X. Jiang, Z. Zhang, X.Z. Kong, Influence of ingredients in water-based polyurethane-acrylic hybrid latexes on latex properties, Prog. Org. Coat. 62 (2008) 251–257, https://doi.org/10.1016/j.porgcoat.2007.12.006.
[97] S. Du, Y. Wang, C. Zhang, X. Deng, X. Luo, Y. Fu, Y. Liu, Self-antibacterial UV-curable waterborne polyurethane with pendant amine and modified by guanidinoacetic acid, J. Mater. Sci. 53 (2017) 215–229, https://doi.org/10.1007/s10853-017-1527-2.
[98] L. Wang, X.J. Lai, S.Y. Ma, Preparation of UV curable waterborne polyurethane and its application in coatings, Adv. Mat. Res. 821–822 (2013) 925–928, https://doi.org/10.4028/www.scientific.net/AMR.821-822.925.
[99] T. Zhang, W. Wu, Y. Mu, A novel nanosilica-reinforced waterborne UV-curable material, Second International Conference on Smart Materials and Nanotechnology in Engineering, International Society for Optics and Photonics (2009) 74936I, https://doi.org/10.1117/12.838653.
[100] K. Li, Y. Shen, G. Fei, H. Wang, C. Wang, The effect of PETA/PETTA composite system on the performance of UV curable waterborne polyurethane acrylate, J. Appl. Polym. Sci. 132 (2015), https://doi.org/10.1002/app.41262.
[101] H. Wang, J. Fan, G. Fei, J. Lan, Z. Zhao, Preparation and property of waterborne UV-curable chain-extended polyurethane surface sizing agent: strengthening and waterproofing mechanism for cellulose fiber paper, J. Appl. Polym. Sci. 132 (2015) 42354, https://doi.org/10.1002/app.42354.
[102] T. Zhang, W.J. Wu, L. Zhang, X.D. Dai, Investigation on properties of a new CB/WPUA composite coating, Adv. Mat. Res. 328–330 (2011) 1610–1613, https://doi.org/10.4028/www.scientific.net/AMR.328-330.1610.
[103] S. Zhang, J. Chen, D. Han, Y. Feng, C. Shen, C. Chang, Z. Song, The effect of soft segment on the microstructure and mechanical properties of waterborne UV-curable polyurethane/silica nanocomposites, J. Polym. Res. 22 (2015), https://doi.org/10.1007/s10965-015-0748-9.
[104] K. Li, Y. Shen, G. Fei, H. Wang, J. Li, Preparation and properties of castor oil/pentaerythritol triacrylate-based UV curable waterborne polyurethane acrylate, Prog. Org. Coat. 78 (2015) 146–154, https://doi.org/10.1016/j.porgcoat.2014.09.012.
[105] C. Li, H. Xiao, X. Wang, T. Zhao, Development of green waterborne UV-curable vegetable oil-based urethane acrylate pigment prints adhesive: preparation and application, J. Clean. Prod. 180 (2018) 272–279, https://doi.org/10.1016/j.jclepro.2018.01.193.
[106] J. Xu, X. Rong, T. Chi, M. Wang, Y. Wang, D. Yang, F. Qiu, Preparation, characterization of UV-curable waterborne polyurethane-acrylate and the application in metal iron surface protection, J. Appl. Polym. Sci. 130 (2013) 3142–3152, https://doi.org/10.1002/app.39539.

[107] Y.T. Dai, F.X. Qiu, J.C. Xu, Z.P. Yu, P.F. Yang, B.B. Xu, Y. Jiang, D.Y. Yang, Preparation and properties of UV-curable waterborne graphene oxide/polyurethane-acrylate composites, Plast. Rubber. Compos. 43 (2014) 54–62, https://doi.org/10.1179/1743289813y.0000000071.
[108] F. Qiu, H. Xu, Y. Wang, J. Xu, D. Yang, Preparation, characterization and properties of UV-curable waterborne polyurethane acrylate/SiO2 coating, J. Coat. Technol. Res. 9 (2012) 503–514, https://doi.org/10.1007/s11998-012-9397-7.
[109] J. Xu, F. Qiu, X. Rong, Y. Dai, D. Yang, Preparation and surface pigment protection application of stone substrate on UV-curable waterborne polyurethane-acrylate coating, J. Polym. Mater. 31 (2014) 287–303.
[110] J. Xu, Y. Jiang, T. Zhang, Y. Dai, D. Yang, F. Qiu, Z. Yu, P. Yang, Fabrication of UV-curable waterborne fluorinated polyurethane-acrylate and its application for simulated iron cultural relic protection, J. Coat. Technol. Res. 15 (2018) 535–541, https://doi.org/10.1007/s11998-017-0009-4.
[111] J. Xu, Y. Jiang, T. Zhang, Y. Dai, D. Yang, F. Qiu, Z. Yu, P. Yang, Synthesis of UV-curing waterborne polyurethane-acrylate coating and its photopolymerization kinetics using FT-IR and photo-DSC methods, Prog. Org. Coat. 122 (2018) 10–18, https://doi.org/10.1016/j.porgcoat.2018.05.008.
[112] Y. Dai, F. Qiu, L. Wang, J. Zhao, Z. Yu, P. Yang, D. Yang, L. Kong, UV-curable electromagnetic shielding composite films produced through waterborne polyurethane-acrylate bonded graphene oxide: preparation and effect of different diluents on the properties, e-Polymers 14 (2014) 427–440, https://doi.org/10.1515/epoly-2014-0163.
[113] Y. Dai, F. Qiu, L. Wang, J. Zhao, D. Yang, L. Kong, Z. Yu, P. Yang, Effect of different photoinitiators on the properties of UV-cured electromagnetic shielding composites, J. Polym. Eng. 35 (2015) 209–222, https://doi.org/10.1515/polyeng-2014-0192.
[114] J. Feng, L. Fang, D. Ye, Self-photoinitiated oligomers of water-diluted polyurethane acrylate grafted with zinc oxide of low concentrations, Prog. Org. Coat. 120 (2018) 208–216, https://doi.org/10.1016/j.porgcoat.2018.04.004.
[115] J. Feng, D. Ye, Polymerizable ZnO photoinitiators of surface modification with hydroxyl acrylates and photopolymerization with UV-curable waterborne polyurethane acrylates, Eur. Polym. J. 120 (2019), 109252, https://doi.org/10.1016/j.eurpolymj.2019.109252.
[116] J. Feng, D. Ye, Self-photoinitiating water-diluted polyurethane acrylates and their UV-curing kinetics, Prog. Org. Coat. 129 (2019) 300–308, https://doi.org/10.1016/j.porgcoat.2019.01.027.
[117] J.G. Gao, F.L. Zhu, J.B. Yang, X.Q. Liu, Synthesis and curing kinetics of UV-curable waterborne bisphenol-S epoxy acrylate/polyurethane-acrylate coating, Adv. Mat. Res. 549 (2012) 457–461, https://doi.org/10.4028/www.scientific.net/AMR.549.457.
[118] Z. Wu, Q. Guo, R.P. Jia, F.W. Liu, Structure and properties of UV-curable waterborne polyurethane/acrylate composite resin, Adv. Mat. Res. 177 (2010) 677–681, https://doi.org/10.4028/www.scientific.net/AMR.177.677.
[119] H.D. Hwang, H.J. Kim, UV-curable low surface energy fluorinated polycarbonate-based polyurethane dispersion, J. Colloid Interface Sci. 362 (2011) 274–284, https://doi.org/10.1016/j.jcis.2011.06.044.
[120] S. Zhang, Z. Chen, M. Guo, J. Zhao, X. Liu, Waterborne UV-curable polycarbonate polyurethane nanocomposites based on polydimethylsiloxane and colloidal silica with enhanced mechanical and surface properties, RSC Adv. 4 (2014) 30938–30947, https://doi.org/10.1039/c4ra03842h.
[121] S.C. Song, S.J. Kim, K.-K. Park, J.-G. Oh, S.-G. Bae, G.H. Noh, W.-K. Lee, Synthesis and properties of waterborne UV-curable polyurethane acrylates using functional isocyanate, Mol. Cryst. Liq. Cryst. 659 (2018) 40–45, https://doi.org/10.1080/15421406.2018.1450824.
[122] S.C. Song, H.H. Choi, K.-K. Park, S. Lee, W.-K. Lee, Synthesis and properties of waterborne polyurethane acrylates using reactive silicone, Mol. Cryst. Liq. Cryst. 688 (2019) 7–13, https://doi.org/10.1080/15421406.2019.1651062.
[123] S. Zhang, Z. Chen, Z. Xu, S. Gang, H. Bai, X. Liu, Hydrophobic, transparent waterborne UV-curable polyurethane nanocomposites based on polycarbonate and PCL-PDMS-PCL reinforced with colloidal silica, J. Coat. Technol. Res. 13 (2016) 1021–1033, https://doi.org/10.1007/s11998-016-9806-4.
[124] Q. Zhang, W. Liu, F. Sun, Synthesis and properties of waterborne UV-curable polydimethylsiloxane-based polyurethane oligomers: UV-cured film with excellent water resistance and thermostability, J. Adhes. Sci. Technol. (2020) 1–17, https://doi.org/10.1080/01694243.2020.1757191.
[125] K.K. Jena, R. Narayan, K.V.S.N. Raju, New high performance waterborne organic–inorganic hybrid materials from UV curing, Prog. Org. Coat. 76 (2013) 1418–1424, https://doi.org/10.1016/j.porgcoat.2013.04.014.
[126] A. Asif, C. Huang, W. Shi, Structure-property study of waterborne, polyurethane acrylate dispersions based on hyperbranched aliphatic polyester for UV-curable coatings, Colloid Polym. Sci. 283 (2004) 200–208, https://doi.org/10.1007/s00396-004-1123-2.
[127] A. Asif, C.Y. Huang, W.F. Shi, Photopolymerization of waterborne polyurethane acrylate dispersions based on hyperbranched aliphatic polyester and properties of the cured films, Colloid Polym. Sci. 283 (2004) 721–730, https://doi.org/10.1007/s00396-004-1212-2.
[128] A. Asif, W. Shi, UV curable waterborne polyurethane acrylate dispersions based on hyperbranched aliphatic polyester: effect of molecular structure on physical and thermal properties, Polym. Adv. Technol. 15 (2004) 669–675, https://doi.org/10.1002/pat.528.
[129] W. Yin, X. Zeng, H. Li, Y. Hou, Q. Gao, Synthesis, photopolymerization kinetics, and thermal properties of UV-curable waterborne hyperbranched polyurethane acrylate dispersions, J. Coat. Technol. Res. 8 (2011) 577–584, https://doi.org/10.1007/s11998-011-9338-x.
[130] W. Yin, X. Zeng, H. Li, X. Lin, B. Ren, Z. Tong, Steady rheological behaviors of UV-curable waterborne hyperbranched polyurethane acrylate dispersions, J. Coat. Technol. Res. 10 (2012) 57–64, https://doi.org/10.1007/s11998-012-9432-8.
[131] A. Asif, L. Hu, W. Shi, Synthesis, rheological, and thermal properties of waterborne hyperbranched polyurethane acrylate dispersions for UV curable coatings, Colloid Polym. Sci. 287 (2009) 1041–1049, https://doi.org/10.1007/s00396-009-2062-8.
[132] X. Lin, S. Zhang, J. Qian, Synthesis and properties of a novel UV-curable waterborne hyperbranched polyurethane, J. Coat. Technol. Res. 11 (2013) 319–328, https://doi.org/10.1007/s11998-013-9520-4.
[133] H. Hu, Y. Yuan, W. Shi, Preparation of waterborne hyperbranched polyurethane acrylate/LDH nanocomposite, Prog. Org. Coat. 75 (2012) 474–479, https://doi.org/10.1016/j.porgcoat.2012.06.007.
[134] K. Liu, Z. Su, S. Miao, G. Ma, S. Zhang, UV-curable enzymatic antibacterial waterborne polyurethane coating, Biochem. Eng. J. 113 (2016) 107–113, https://doi.org/10.1016/j.bej.2016.06.004.
[135] N. Hao, J. Wu, J. Wan, Z. Liu, Morphology and mechanical properties of UV-curable castor oil-based waterborne polyurethane/organic montmorillonite nanocomposites, Plast. Rubber. Compos. 46 (2017) 346–354, https://doi.org/10.1080/14658011.2017.1356974.
[136] D. Wei, B. Liao, Q. Yong, H. Wang, T. Li, J. Huang, H. Pang, Castor oil-based waterborne hyperbranched polyurethane acrylate emulsion for UV-curable coatings with excellent chemical resistance and high hardness, J. Coat. Technol. Res. 16 (2018) 415–428, https://doi.org/10.1007/s11998-018-0120-1.
[137] V. Mishra, I. Mohanty, M.R. Patel, K.I. Patel, Development of green waterborne UV-curable castor oil-based urethane acrylate coatings: preparation and property analysis, Int. J. Polym. Anal. Charact. 20 (2015) 504–513, https://doi.org/10.1080/1023666x.2015.1050852.
[138] C.-W. Chang, K.-T. Lu, Linseed-oil-based waterborne UV/air dual-cured wood coatings, Prog. Org. Coat. 76 (2013) 1024–1031, https://doi.org/10.1016/j.porgcoat.2013.02.020.
[139] V. Mishra, J. Desai, K.I. Patel, (UV/Oxidative) dual curing polyurethane dispersion from cardanol based polyol: synthesis and characterization, Ind. Crops Prod. 111 (2018) 165–178, https://doi.org/10.1016/j.indcrop.2017.10.015.
[140] Y. Zhang, A. Asif, W. Shi, Highly branched polyurethane acrylates and their waterborne UV curing coating, Prog. Org. Coat. 71 (2011) 295–301, https://doi.org/10.1016/j.porgcoat.2011.03.022.
[141] C. Yuan, M. Wang, H. Li, Z. Wang, Preparation and properties of UV-curable waterborne polyurethane-acrylate emulsion, J. Appl. Polym. Sci. 134 (2017) 45208, https://doi.org/10.1002/app.45208.
[142] I. Etxaniz, O. Llorente, J. Aizpurua, L. Martín, A. González, L. Irusta, Dispersion characteristics and curing behaviour of waterborne UV crosslinkable polyurethanes based on renewable dimer fatty acid polyesters, J. Polym. Environ. 27 (2018) 189–197, https://doi.org/10.1007/s10924-018-1334-0.
[143] Z. Yang, D.A. Wicks, C.E. Hoyle, H. Pu, J. Yuan, D. Wan, Y. Liu, Newly UV-curable polyurethane coatings prepared by multifunctional thiol- and ene-terminated polyurethane aqueous dispersions mixtures: Preparation and characterization, Polymer 50 (2009) 1717–1722, https://doi.org/10.1016/j.polymer.2008.12.018.
[144] Z. Yang, D.A. Wicks, J. Yuan, H. Pu, Y. Liu, Newly UV-curable polyurethane coatings prepared by multifunctional thiol- and ene-terminated polyurethane aqueous dispersions: photopolymerization properties, Polymer 51 (2010) 1572–1577, https://doi.org/10.1016/j.polymer.2010.02.003.
[145] Z.X. Wang, J.L. Wang, Q.L. Liu, J.T. Yuan, H. Chen, UV curable polyurethane dispersions extended by a new chain extender, Adv. Mat. Res. 904 (2014) 137–141, https://doi.org/10.4028/www.scientific.net/AMR.904.137.
[146] D.B. Otts, E. Heidenreich, M.W. Urban, Novel waterborne UV-crosslinkable thiol–ene polyurethane dispersions: synthesis and film formation, Polymer 46 (2005) 8162–8168, https://doi.org/10.1016/j.polymer.2005.06.075.
[147] W.C. Lin, C.H. Yang, T.L. Wang, Y.T. Shieh, W.J. Chen, Hybrid thin films derived from UV-curable acrylate-modified waterborne polyurethane and monodispersed colloidal silica, Express Polym. Lett. 6 (2012) 2–13, https://doi.org/10.3144/expresspolymlett.2012.2.
[148] V.K. Mishra, K.I. Patel, Nonionic diol modified UV-curable polyurethane dispersions: preparation and characterization, J. Dispers. Sci. Technol. 36 (2014) 351–362, https://doi.org/10.1080/01932691.2014.903805.
[149] V. Mishra, J. Desai, K.I. Patel, High-performance waterborne UV-curable polyurethane dispersion based on thiol–acrylate/thiol–epoxy hybrid networks, J. Coat. Technol. Res. 14 (2017) 1069–1081, https://doi.org/10.1007/s11998-016-9906-1.
[150] L. Zhang, H. Zhang, J. Guo, Synthesis and properties of UV-curable polyester-based waterborne polyurethane/functionalized silica composites and morphology of their nanostructured films, Ind. Eng. Chem. Res. 51 (2012) 8434–8441, https://doi.org/10.1021/ie3000248.
[151] K. Wu, S. Xiang, W. Zhi, R. Bian, C. Wang, D. Cai, Preparation and characterization of UV curable waterborne poly(urethane-acrylate)/antimony doped tin oxide thermal insulation coatings by sol-gel process, Prog. Org. Coat. 113 (2017) 39–46, https://doi.org/10.1016/j.porgcoat.2017.08.004.
[152] H. Yu, Q. Yuan, D. Wang, Y. Zhao, Preparation of an ultraviolet-curable waterborne poly(urethane acrylate)/silica dispersion and properties of its hybrid film, J. Appl. Polym. Sci. 94 (2004) 1347–1352, https://doi.org/10.1002/app.20694.
[153] C. Decker, F. Masson, R. Schwalm, Weathering resistance of waterbased UV-cured polyurethane-acrylate coatings, Polym. Degrad. Stab. 83 (2004) 309–320, https://doi.org/10.1016/s0141-3910(03)00276-3.
[154] Q.-A. Li, D.-C. Sun, Synthesis and characterization of high solid content aqueous polyurethane dispersion, J. Appl. Polym. Sci. 105 (2007) 2516–2524, https://doi.org/10.1002/app.24627.

[155] X. Zhou, Y. Hao, X. He, D. Zhou, L. Xie, S. Liu, B. Qiao, Protean morphology of waterborne polyurethane dispersion: an overview of nanoparticles from sphere to irregular elongated shape, Prog. Org. Coat. 146 (2020), 105742, https://doi.org/10.1016/j.porgcoat.2020.105742.
[156] F. Bao, W. Shi, Synthesis and properties of hyperbranched polyurethane acrylate used for UV curing coatings, Prog. Org. Coat. 68 (2010) 334–339, https://doi.org/10.1016/j.porgcoat.2010.03.002.
[157] Q. Chen, X. Du, G. Chen, A green method of reducing silver nanoparticles based on bagasse pulp extract for preparing ultraviolet (UV)-curable conductive ink, J. Vinyl Addit. Technol. 26 (2019) 90–96, https://doi.org/10.1002/vnl.21718.
[158] Y. Okamoto, Y. Hasegawa, F. Yoshino, Urethane/acrylic composite polymer emulsions, Prog. Org. Coat. 29 (1996) 175–182, https://doi.org/10.1016/s0300-9440(96)00660-1.
[159] J. Tan, W. Liu, H. Wang, Y. Sun, S. Wang, Preparation and properties of UV-curable waterborne comb-like (meth)acrylate copolymers with long fluorinated side chains, Prog. Org. Coat. 94 (2016) 62–72, https://doi.org/10.1016/j.porgcoat.2016.01.027.
[160] H. Liang, C. Lv, L. Xiong, S. Huang, H. Fan, Synthesis and characterization of novel UV-curable waterborne fluorinated polyurethane acrylate latex, Asian J. Chem. 26 (2014) 350–352, https://doi.org/10.14233/ajchem.2014.15381.
[161] C. Decker, F. Masson, R. Schwalm, How to speed up the UV curing of water-based acrylic coatings, J. Coat. Technol. Res. 1 (2004) 127–136, https://doi.org/10.1007/s11998-004-0007-1.
[162] C. Sow, B. Riedl, P. Blanchet, Kinetic studies of UV-waterborne nanocomposite formulations with nanoalumina and nanosilica, Prog. Org. Coat. 67 (2010) 188–194, https://doi.org/10.1016/j.porgcoat.2009.10.002.
[163] G. Baysal, B. Kalav, B. Karagüzel Kayaoğlu, Colour and gloss properties of pigment-printed synthetic leather using an ultraviolet-curable water-borne polyurethane acrylate binder and two photoinitiators at different ratios, Color. Technol. 135 (2019) 133–142, https://doi.org/10.1111/cote.12386.
[164] M. Yamamoto, G. Oster, Zinc oxide-sensitized photopolymerization, J. Polym. Sci. A-1 4 (1966) 1683–1688, https://doi.org/10.1002/pol.1966.150040703.
[165] F. Masson, C. Decker, T. Jaworek, R. Schwalm, UV-radiation curing of waterbased urethane-acrylate coatings, Prog. Org. Coat. 39 (2000) 115–126, https://doi.org/10.1016/s0300-9440(00)00128-4.
[166] D. Dieterich, Aqueous emulsions, dispersions and solutions of polyurethanes; synthesis and properties, Prog. Org. Coat. 9 (1981) 281–340, https://doi.org/10.1016/0033-0655(81)80002-7.
[167] K.J. van den Berg, L.G.J. van der Ven, H.J.W. van den Haak, Development of waterborne UV-A curable clear coat for car refinishes, Prog. Org. Coat. 61 (2008) 110–118, https://doi.org/10.1016/j.porgcoat.2007.09.037.
[168] H.-D. Hwang, J.-I. Moon, J.-H. Choi, H.-J. Kim, S.D. Kim, J.C. Park, Effect of water drying conditions on the surface property and morphology of waterborne UV-curable coatings for engineered flooring, J. Ind. Eng. Chem. 15 (2009) 381–387, https://doi.org/10.1016/j.jiec.2008.11.002.
[169] J.F.G.A. Jansen, A.A. Dias, M. Dorschu, B. Coussens, Fast monomers: factors affecting the inherent reactivity of acrylate monomers in photoinitiated acrylate polymerization, Macromolecules 36 (2003) 3861–3873, https://doi.org/10.1021/ma021785r.
[170] S.C. Ligon, B. Husar, H. Wutzel, R. Holman, R. Liska, Strategies to reduce oxygen inhibition in photoinduced polymerization, Chem. Rev. 114 (2014) 557–589, https://doi.org/10.1021/cr3005197.
[171] C. Belon, X. Allonas, C. Croutxé-barghorn, J. Lalevée, Overcoming the oxygen inhibition in the photopolymerization of acrylates: a study of the beneficial effect of triphenylphosphine, J. Polym. Sci. Part A: Polym. Chem. 48 (2010) 2462–2469, https://doi.org/10.1002/pola.24017.
[172] N. Wang, L. Zhang, J. Gu, Mechanical properties and biodegradability of crosslinked soy protein isolate/waterborne polyurethane composites, J. Appl. Polym. Sci. 95 (2005) 465–473, https://doi.org/10.1002/app.21237.
[173] T.J. Lee, S.H. Kwon, B.K. Kim, Biodegradable sol–gel coatings of waterborne polyurethane/gelatin chemical hybrids, Prog. Org. Coat. 77 (2014) 1111–1116, https://doi.org/10.1016/j.porgcoat.2014.03.011.
[174] M.E.V. Hormaiztegui, V.L. Mucci, A. Santamaria-Echart, M.A. Corcuera, A. Eceiza, M.I. Aranguren, Waterborne polyurethane nanocomposites based on vegetable oil and microfibrillated cellulose, J. Appl. Polym. Sci. 133 (2016) 44207, https://doi.org/10.1002/app.44207.
[175] O.I. Negru, L. Vacareanu, M. Grigoras, Electrogenerated networks from poly [4-(diphenylamino)benzyl methacrylate] and their electrochromic properties, Express Polym. Lett. 8 (2014) 647–658, https://doi.org/10.3144/expresspolymlett.2014.68.
[176] C. Fu, X. Hu, Z. Yang, L. Shen, Z. Zheng, Preparation and properties of waterborne bio-based polyurethane/siloxane cross-linked films by an in situ sol–gel process, Prog. Org. Coat. 84 (2015) 18–27, https://doi.org/10.1016/j.porgcoat.2015.02.008.
[177] Z. Liang, J. Zhu, F. Li, Z. Wu, Y. Liu, D. Xiong, Synthesis and properties of self-crosslinking waterborne polyurethane with side chain for water-based varnish, Prog. Org. Coat. 150 (2021), 105972, https://doi.org/10.1016/j.porgcoat.2020.105972.